Electronic Supplementary Material (ESI) for Chemical Science

Straightforward access to *bis*benzamidine dsDNA binders and their use as versatile adaptors for DNA-promoted processes

Mateo I. Sánchez, Olalla Vázquez, José Martínez-Costas, M. Eugenio Vázquez and José L. Mascareñas**

Departamento de Química Orgánica, Centro Singular de Investigación en Química Biolóxica e Materiais Moleculares, y Unidad Asociada ao CSIC. Universidade de Santiago de Compostela. 15782 Santiago de Compostela (Spain). Fax : (+ 34) 881 81 44 05. E-mail: joseluis.mascarenas@usc.es; or eugenio.vazquez@usc.es

Departamento de Bioquímica e Bioloxía Molecular, Centro Singular de Investigación en Química Biolóxica e Materiais Moleculares. Universidade de Santiago de Compostela. 15782 Santiago de Compostela (Spain).

UV Spectroscopy. The molar extinction coefficients of compounds **4**, **7**, **8**, **9**, **10**, **11**, **12**, **13** and a control triazole derivative (**16**), isolated as TFA disalts, were obtained by linear regression analysis of the UV absorption values of samples of known concentrations by weight. **4**, ε_{314} = 29,636 M^{-1} cm^{-1}; **7**, ε_{311} = 47,705 M^{-1} cm^{-1}; **8**, ε_{311} = 43757 M^{-1} cm^{-1}; **9**, ε_{314} = 37,961 M^{-1} cm^{-1}; **10**, ε_{314} = 40,397 M^{-1} cm^{-1}; **11**, ε_{311} = 39,455 M^{-1} cm^{-1}; **12**, ε_{311} = 31,402 M^{-1} cm^{-1}; **13**, ε_{311} = 50,234 M^{-1} cm^{-1}; **16**, ε_{311} = 33,259 M^{-1} cm^{-1}. Extinction coefficients of **15b** and **15c** were assumed the same as that of the control compound **16**. Extinction coefficients used for the compounds **15a** and **14a** are the same as the described ones for 7-diethylaminocoumarin-3-carboxylic acid. The molar extinction coefficients of hairpin oligonucleotides were calculated with the following formula: ε_{260} = [(8.8 × #T) + (7.3 × #C) + (11.7 × #G) + (15.4 × #A)] × 0.8· 10^3 M^{-1} cm^{-1}. Where, #T, #C, #G and #A are the number bases of each type in the sequence.[1]

Synthesis. DMF and TFA were from *Scharlau*, CH_2Cl_2 from *Panreac*, CH_3CN from *Merck*. The rest of reagents were acquired from *Sigma-Aldrich* and *Invitrogen*. Some reactions were followed by analytical RP-HPLC with an Agilent 1100 series LC/MS using an Eclipse XDB-C_{18} (4.6 x 150 mm, 5 µm) analytical column. Standard conditions for analytical RP-HPLC consisted on an isocratic regime during the first 5 min, followed by a linear gradient from 5% to 95% of solvent B for 30 min at a flow rate of 1 mL/min (A: water with 0.1% TFA, B: acetonitrile with 0.1% TFA). Final products were purified on a *Büchi* Sepacore preparative system consisting on a pump manager C-615 with two pump modules C-605 for binary solvent gradients, a fraction collector C-660, and UV Photometer C-635. Purification was made using reverse phase linear gradients of MeCN/H_2O, with 0.1% TFA in 30 min with a flow rate of 30 mL/min, using a pre-packed preparative cartridge (150 × 40 mm) with reverse phase RP18ec silica gel (*Büchi* order number 54863). The fractions containing the products were freeze-dried, and their identity was confirmed by ESI-MS. All the bis-benzamidines were purified by HPLC and isolated as bis-TFA salts.

4-({5-[(4-carbamimidoylphenyl)amino]pentyl}amino) benzene-1-carboximidamide (4). 4-Aminobenzamidine dihydrochloride (312 mg, 1.5 mmol) and sodium cyanoborohydride (24 mg, 0.37 mmol) were dissolved in a round bottom flask in 2 mL of aqueous buffer (NaH_2PO_4/Na_2HPO_4 100 mM pH = 8.3) with magnetic stirring. Glutaric dialdehyde (25 mg, 0.25 mmol, 50 wt. % solution in water) was added dropwise. After 30 min the solvents were removed under reduced pressure, and the resulting residue was purified by preparative reverse-phase chromatography. The combined fractions were concentrated and freeze-dried yielding a white solid that was identified as the desire product as a bis-trifluoroacetic salt (27 mg, 0.05 mmol, 17%). ^{1}H-RMN: (500MHz, DMSO-d^6 δ) 1.45 (td, *J* = 15.2, 7.5 Hz, 2H), 1.64-1.54 (m, 4H), 3.11 (t, *J* = 6.9 Hz, 4H), 6.66 (d, *J* = 8.9 Hz, 4H), 6.81 (broad s, 2H) 7.64 (d, *J* = 8.9 Hz, 4H), 8.62 (s, 4H), 8.76 (s, 4H). ^{13}C-RMN: 24.1 (CH_2), 28.2 (CH_2), 42.1 (CH_2), 110.9 (C), 111.9 (CH), 129.7 (CH), 153.6 (C), 164.2 (C). ESI+-MS: $[M+H]^+$ calcd. for $C_{19}H_{27}N_6$ = 339.2292 found 339.2284.

(1) a) Engman, K. C.; Sandin, P.; Osborne, S.; Brown, T.; Billeter, M.; Lincoln, P.; Nordén, B.; Albinsson, B.; Wilhelmsson. L. M. *Nucl. Acids Res.* **2004**, *17*, 5087-5095. b) Kallansrud, G.; Ward. B. *Anal Biochem.* **1996**, *236*, 134-138.

General method for the synthesis of bisbenzamidines.

Synthesis of 4-{[(3-{[(4-carbamimidoylphenyl)amino] methyl}phenyl) methyl]amino}benzene-1-carboximidamide (7). Isopthaldehyde (150 mg, 1.1 mmol), 4-aminobenzamidine dihydrochloride (508 mg, 2.4 mmol), and sodium cyanoborohydride (104 mg, 1.65 mmol) were added to a round bottom flask and dissolved in 11 mL of MeCN/H_2O 1:1. The reaction mixture was stirred under Ar at room temperature for 30 min. The solvents were removed under reduced pressure and the resulting residue was purified by preparative reverse-phase chromatography. The combined fractions were concentrated and freeze-dried yielding a white solid that was identified as the bis-trifluoroacetic salt of the desired product (512 mg, 77%). ^{1}H-RMN (300 MHz, DMSO-d^6 δ): 4.36 (s, 4H), 6.68 (d, J = 8.9 Hz, 4H), 7.31-7.34 (m, 4H), 7.60 (d, J = 8.9 Hz, 4H), 8.61 (s, 4H), 8.77 (s, 4H). ^{13}C-RMN: 45.7 (CH_2), 111.4 (C), 112.6 (CH), 125.7 (CH), 126.0 (CH), 128.5 (CH), 129.6 (CH), 139.2 (C), 153.3 (C), 158.3 (C, TFA). 164.2 (C). ESI-MS: $[M+H]^+$ calcd. for $C_{22}H_{24}N_6$ = 373.2135 found 373.2133.

4-{[(4-{[(4-carbamimidoylphenyl)amino]methyl}phenyl) methyl]amino}benzene-1-carboximidamide (8). Same procedure as for the synthesis of **7**, starting from terepthaldehyde. ^{1}H RMN (400 MHz, DMSO-d^6 δ): 4.34 (s, 4H), 6.67 (d, J = 8.8 Hz, 4H), 7.29 (s, 4H), 7.57 (d, J = 8.9 Hz, 1H), 8, 40 (s, 4 H), 8.75 (s, 4H). ^{13}C RMN: 45.4 (CH_2), 111.6 (CH), 112.6 (C), 127.4 (CH), 129.8 (CH), 137.8 (C), 153.4 (C), 158.4 (C, TFA) 163.3 (C). ESI-MS: $[M+H]^+$ calcd. for $C_{22}H_{24}N_6$ = 373.2135 found 373.2133.

3,5-bis({[(4-carbamimidoylphenyl)amino]methyl}) phenyl]boronic acid (9). Same procedure as for the synthesis of **7**, starting from 3,5-diformylphenyl boronic acid. ^{1}H RMN (500 MHz, DMSO-d^6 δ): 4.33 (s, 4H), 6.68 (d, J = 8.9 Hz, 4H), 7.36 (s, 1H), 7.60 (d, J = 8.9 Hz, 4H), 7.67 (broad s, 2H), 8.55 (s, 4H), 8.76 (s, 4H). ^{13}C RMN: 46.0 (CH_2), 111.4 (CH), 112.5 (C), 127.9 (CH), 129, 6 (broad s, CH), 129.6 (broad s, C, C-B$(OH)_2$), 131.9 (CH), 138.0 (C), 153.3 (C), 158.8 (C, TFA), 164.2 (C). ESI-MS: $[M+H]^+$ calcd. for $C_{22}H_{26}BN_6O_2$ = 417.2209 found 417.2208.

4-{[(6-{[(4-carbamimidoylphenyl)amino]methyl}pyridin-2-yl)methyl]amino}benzene-1-carboximidamide (10). Same procedure as for the synthesis of **7**, starting from 2,6-pyridinedicarboxaldehyde. ^{1}H NMR (400 MHz, DMSO-d^6 δ): 4.48 (s, 4H), 6.72 (d, J = 8.2 Hz, 4H), 7.21 (d, J = 7.7 Hz, 2H), 7.72 (t, J = 7.7 Hz, 1H), 7.61 (d, J = 7.9 Hz, 4H), 8.56 (s, 4H), 8.77 (s, 4H). 13C RMN: 47.6 (CH_2), 111.5 (CH), 113.0 (C), 119.5 (CH), 129.7 (CH), 137.7 (CH), 153.2 (C), 158.1 (C), 158.4 (C, TFA) 164.2 (C). ESI-MS: $[M+H]^+$ calcd. for $C_{21}H_{24}N_7$ = 374.288 found 374.2098.

4-{[(3-{[(4-carbamimidoylphenyl)amino]methyl}-5-hy-droxyphenyl)methyl]amino}benzene-1-carboximidamide, (11). Same procedure as for the synthesis of **7**, starting from 5-hydroxybenzene-1,3-dialdehyde. ^{1}H NMR (300 MHz, DMSO-d^6 δ): 4.27 (d, J = 5.0 Hz, 4H), 6,61 (s, 2H) 6.67 (d, J = 8.9 Hz, 4H), 6,77 (s, 1H) 7.36 (t, J = 5.6 Hz, 2H), 7.60 (d, J = 8.9 Hz, 4H), 8.61 (s ,4H), 8.77 (s, 4H). ^{13}C NMR: 45.7 (CH_2), 111.4 (CH), 112.4 (CH), 112.5 (C), 116.4 (CH), 129.6 (CH), 140.7 (C), 153.4 (C), 157.6 (C), 158.1 (C, TFA), 164.2 (C). ESI-MS: $[M+H]^+$ calcd. for $C_{22}H_{25}N_6O$ = 389.2084 found 389.2098.

4-{[(5-{[(4-carbamimidoylphenyl)amino]methyl}furan-2-yl)methyl]amino}benzene-1-carboximidamide (12). Same procedure as for the synthesis of **7**, starting from furan-2,5-dicarbaldehyde (**12a**). ^{1}H NMR (300 MHz, DMSO-d^6 δ): 4.33 (s, 4H), 6.27 (s, 2H), 6.76 (d, J = 8.9 Hz, 4H), 7.25 (broad s, 2H) 7.63 (d, J = 8.9 Hz, 4H), 8.66 (s, 4H), 8.80 (s, 4H). ^{13}C RMN: 40.8 (CH_2), 108.7 (C), 112.1 (CH), 113.6 (CH), 130.4 (CH), 152.1 (C), 153.7 (C), 158.9 (C, TFA), 164.9 (C). ESI-MS: $[M+H]^+$ calcd. for $C_{20}H_{23}N_6O$ = 363.1928 found 363.1922.

Furan-2,5-dicarbaldehyde (12a)

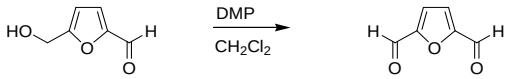

(12a)

A solution of DMP (732 mg, 1.72 mmol) in 7.3 mL of methylene chloride was added to a solution of 5(hydroxymethyl)-2-furaldehyde (181 mg, 1.44 mmol), in 5 mL of methylene chloride with stirring. After 30 min the reaction mixture is diluted with Et_2O (30 mL) and poured into saturated aqueous $NaHCO_3$ (20 mL) containing a sevenfold excess of $Na_2S_2O_3$. The mixture was stirred until the solid has dissolved, and the organic layer was separated and washed with saturated $NaHCO_3$ (1 × 10 mL) and with water (1 × 10 mL). The solvent was removed under reduced pressure and the crude was purified by flash column chromatography on silica gel (40% AcOEt/Hex) to obtain a pale yellow solid that was identified as the desired dialdehyde (134 mg, 1.08 mmol, 78 %). ^{1}H NMR (250 MHz,*CDCl$_3$*): 7.32 (s, 2H), 9.82 (s, 2H). ^{13}C RMN: 119.4 (CH), 154.1 (C), 179.2 (CH). ESI$^+$-MS: [M+H] calc. for $C_6H_5O_3$ = 125.0233 found 125.9230; $C_6H_4O_3$ (M.W. 124.094).

1-[3,5-bis({[(4-carbamimidoylphenyl)amino]methyl}) phenyl]triaza-1,2-dien-2-ium (13). Boronic acid derivative **9** (85 mg, 0.13 mmol), sodium azide (10 mg, 0.16 mmol) and $CuSO_4$ (2 mg, 0.013 mmol) were added to a round bottom flask and dissolved in 2.6 mL of MeOH. The resulting mixture was stirred at rt for 10 hours. The solvent was removed under reduced pressure and the residue was purified by preparative reverse-phase chromatography. The combined fractions were concentrated and freeze-dried, yielding a white solid that was identified as the desire product as a bis-trifluoroacetic salt (74 mg, 0.12 mmol, 86%). ^{1}H RMN (500 MHz, DMSO-*d*^{6} δ): 4.37 (d, *J* = 5.9 Hz, 4H), 6.68 (d, *J* = 8.9 Hz, 4H), 6.98 (s, 2H), 7.18 (s, 1H), 7.39 (t, *J* = 6.1 Hz, 2H), 7.60 (d, *J* = 8.9 Hz, 4H), 8.53 (s, 4H), 8.57 (s, 4H). ^{13}C RMN: 45.3 (CH_2), 111.6 (CH), 113.0 (C), 116.3(CH), 122.8 (CH), 129.8 (CH), 139.7 (C), 141.9 (C), 153.2 (C), 158.4 (C, TFA), 164.3 (C). ESI-MS: [M+H]$^+$ calcd. for $C_{22}H_{24}N_9$ = 414.2149 found 414.2145.

Prop-2-yn-1-yl 7-(diethylamino)-2oxo-2H-chromene-3-carboxylate (14a)

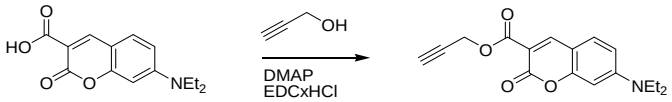

(14a)

A solution of the propargyl alcohol (16 mg, 0.29 mmol) and DMAP (13 mg, 0.11 mmol) in DMF (382 µL) was added to a previous solution of 7-diethylaminocoumarin-3-carboxylic acid (25 mg, 0.1 mmol) and EDC×HCl (27 mg, 0.144 mmol) in DMF (383 µL). The resulting mixture was stirred for 2 h at room temperature until TLC control indicates full conversion. The crude was concentrated under reduced pressure and purified by flash column chromatography on silica gel (5% MeOH/ CH_2Cl_2) to obtain the desired coumarin derivative **14a** (21 mg, 0.072 mmol, 75%). ^{1}H RMN: (300 MHz, *DCCl$_3$ δ*) 1.23 (t, *J* = 7.1 Hz, 6H), 2.50 (t, *J* = 2.5 Hz, 1H), 3.44 (q, *J* = 7.1 Hz, 4H), 4.90 (d, *J* = 2.5 Hz, 2H), 6.45 (d, *J* = 2.4 Hz, 1H), 6.60 (dd, *J* = 9.0, 2.5 Hz, 1H), 7.35 (d, *J* = 9.0 Hz, 1H), 8.46 (s, 1H). ^{13}C RMN: 12.3 (CH_3), 45.1 (CH_2), 52.3 (CH_2), 74.9 (CH), 77.8 (C), 96.6 (CH), 107.5 (C), 107.6 (C), 109.6 (CH), 131.2 (CH), 149.7 (CH), 153.1 (C), 157.9 (C), 158.6 (C), 163.2 (C). ESI$^+$-MS: [M+H] calc. for $C_{17}H_{17}NO_4Na$ = 322.1040 found 322.1050; $C_{17}H_{17}NO_4$ (M.W. 299,321)

1-[3,5-bis({[(4-carbamimidoylphenyl)amino]methyl}) phenyl]-1H-1,2,3-triazol-4-yl 7-(diethylamino)-2-oxo-2H-chromene-3-carboxylate (15a). Alkyne **14a** (21 mg, 0.072 mmol) and azide **13** (88 mg, 0.14 mmol) were dissolved in 2.9 mL of water/DMSO 1:1. $CuSO_4 \times 5\ H_2O$ (3.6 mg, 0.015 mmol), and sodium L-ascorbate (14.2 mg, 0.072 mmol) were added. After stirring for 24 h under Ar at rt, the reaction mixture was directly purified by preparative reverse-phase chromatography. The combined fractions were concentrated and freeze-dried, yielding a bright yellow solid that was identified as the bis-trifluoroacetic salt of the desire product (50 mg, 0.06 mmol, 74%). ^{1}H RMN: (400 MHz, DMSO-d^6 δ) 1.13 (t, J = 7.0 Hz, 6H), 3.48 (dd, J = 14.0, 7.0 Hz, 4H), 4.47 (d, J = 2.7 Hz, 4H), 5.38 (s, 2H), 6.53 (d, J = 2.2 Hz, 1H), 6.72 (d, J = 8.9 Hz, 4H), 6.77 (dd, J = 9.1, 2.37 Hz, 1H), 7.49 (s, 1H), 7.52 (m, 2H) 7.63 (d, J = 8.9 Hz, 4H), 7.64 (d, J = 9.1 Hz, 1H), 7.83 (s, 2H), 8.59 (s, 1H), 8.65 (s, 4H), 8.84 (s, 4H), 8.87 (s, 1H). ^{13}C RMN: 12.3 (CH_3), 44.3 (CH_2), 45.4 (CH_2), 57.3 (CH_2), 95.7 (CH), 106.3 (C), 107.0 (C), 109.9 (CH), 111.6 (CH), 112.9 (C), 117.5 (CH), 123.1 (CH), 126.1 (CH), 129.7 (CH), 131.9 (CH), 136.7 (C), 141.8 (C), 143.3 (C), 149.6 (CH), 153.0 (C), 153.1 (C), 156.9 (C), 158.1 (C), 162.9 (C), 164.3 (C). ESI-MS: $[M+H]^+$ calcd. for $C_{39}H_{41}N_{10}O_4$ = 713.3307 found 713.3307.

NMR SPECTRA

4-({5-[(4- carbamimidoylphenyl)amino]pentyl}amino)benzene-1-carboximidamide. (4)

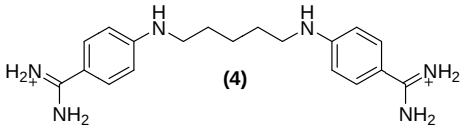

(4)

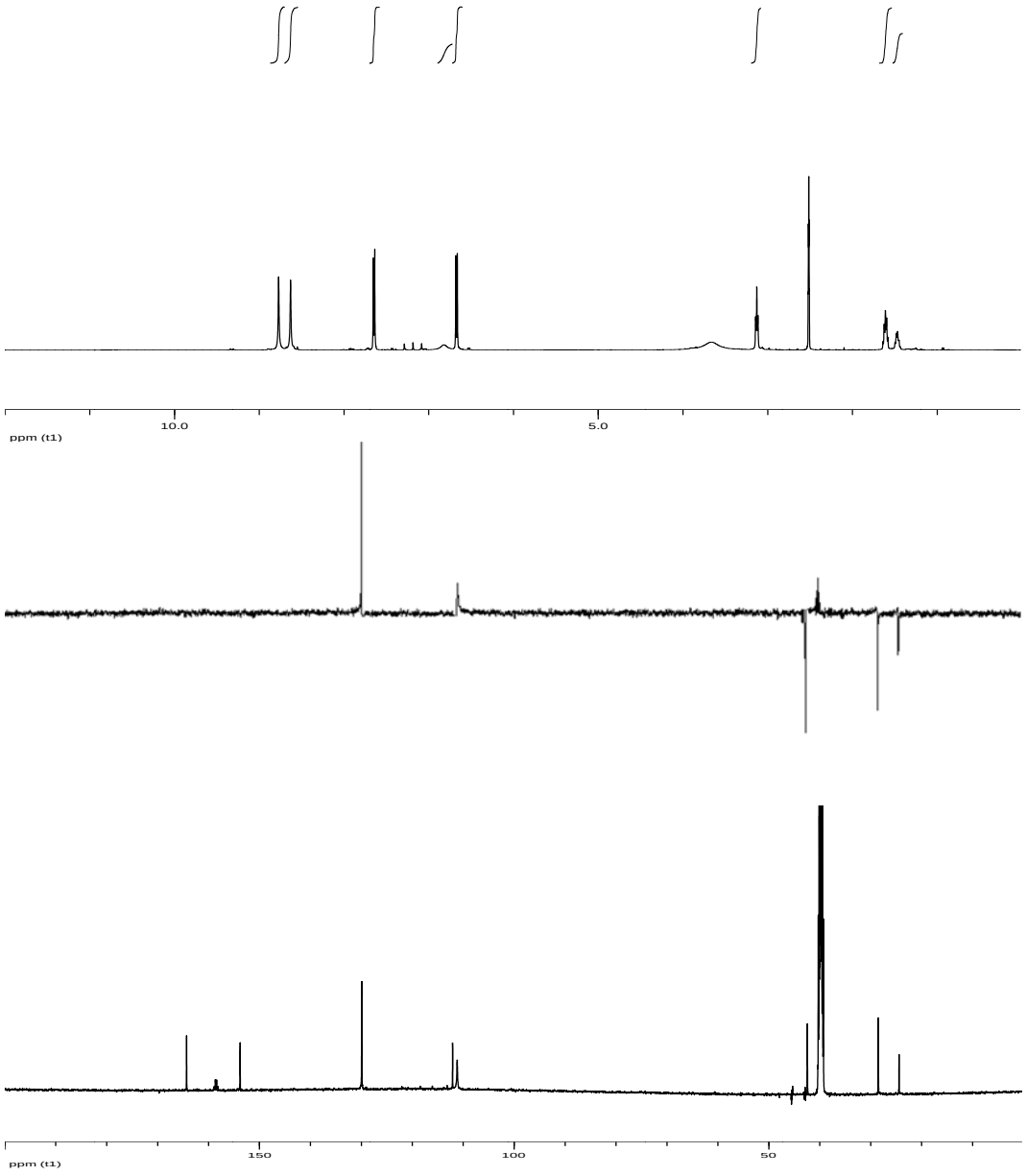

4-{[(3-{[(4-carbamimidoylphenyl)amino]methyl}phenyl)methyl]amino}benzene-1-carboximidamide (7)

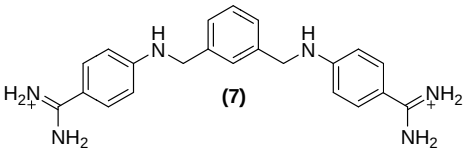

(7)

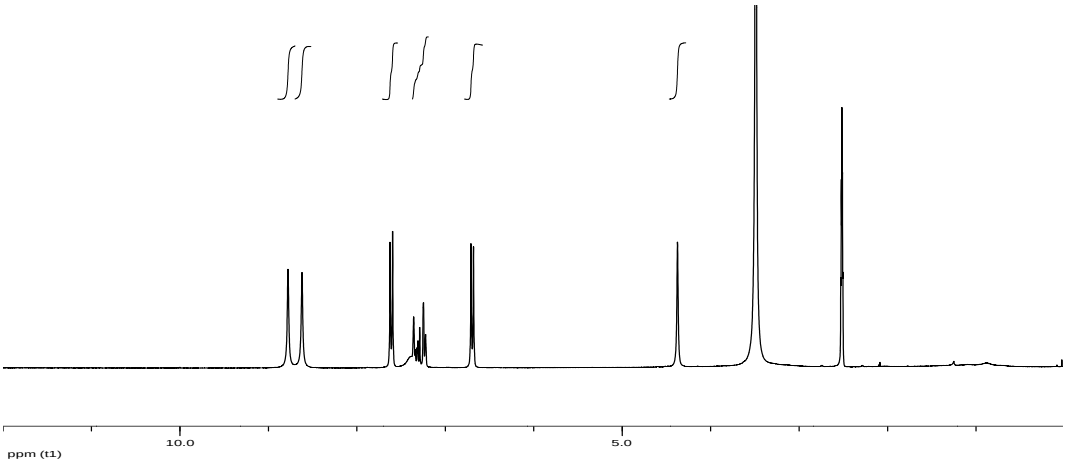

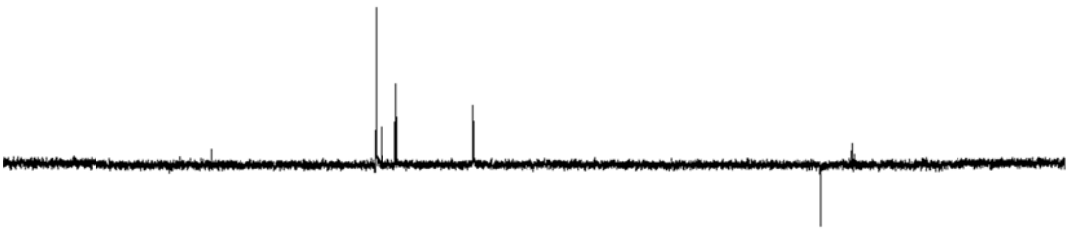

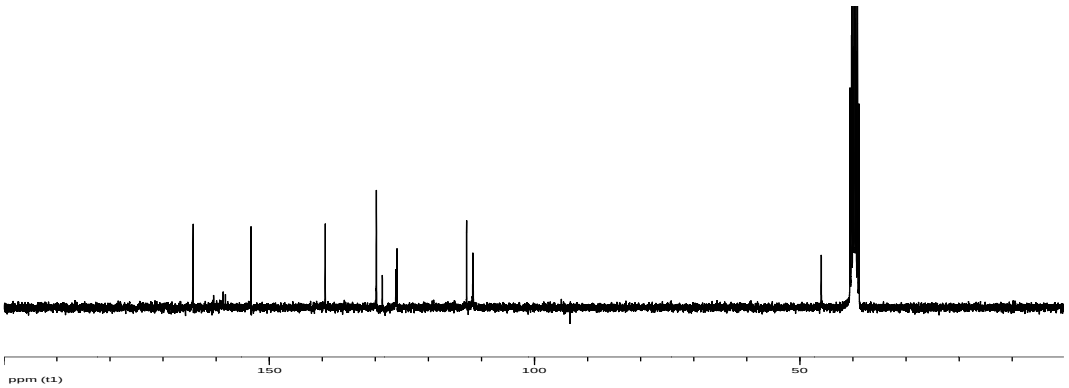

4-{[(4-{[(4-carbamimidoylphenyl)amino]methyl}phenyl)methyl]amino}benzene-1-carboximidamide (8)

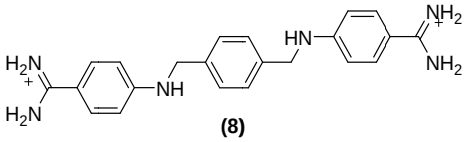

(8)

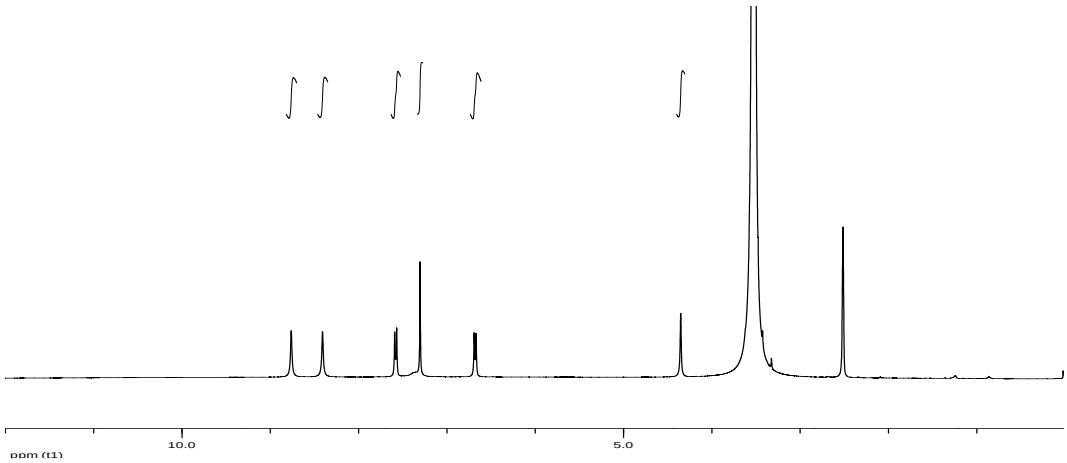

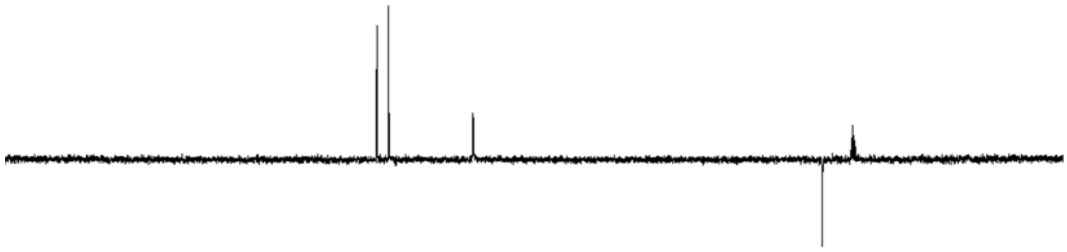

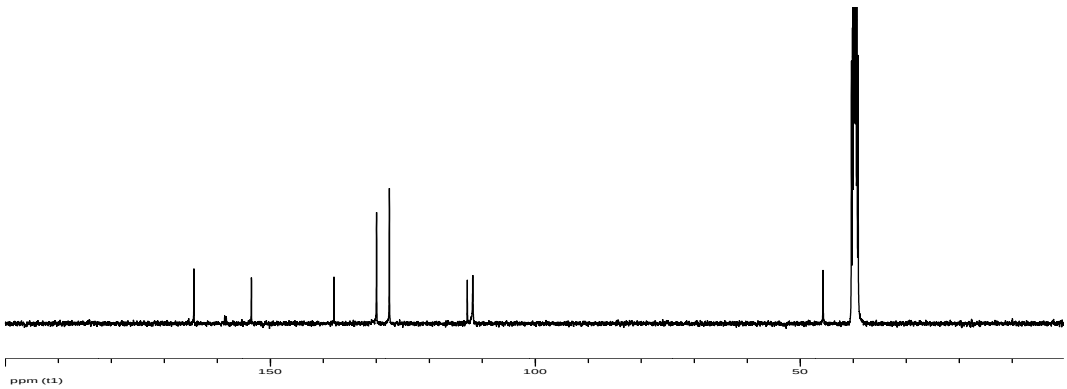

3,5-bis({[(4-carbamimidoylphenyl)amino]methyl})phenyl]boronic acid (9)

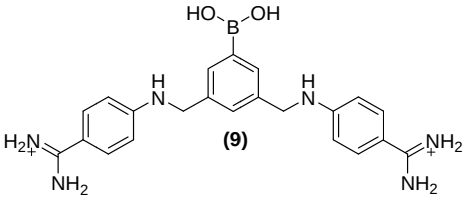

(9)

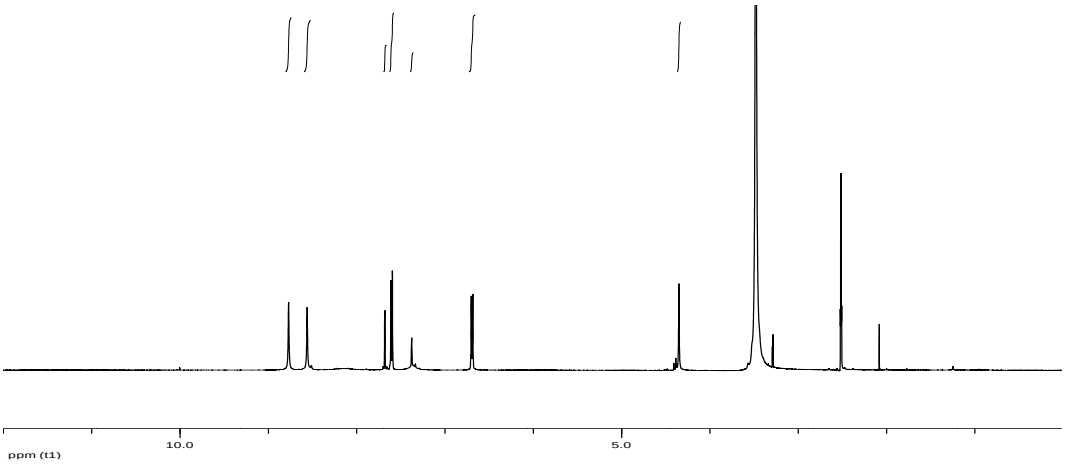

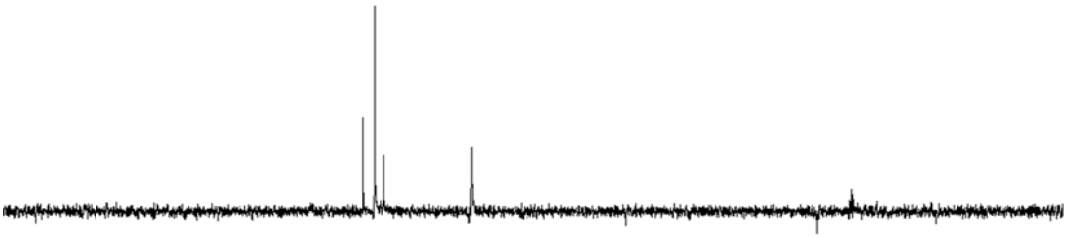

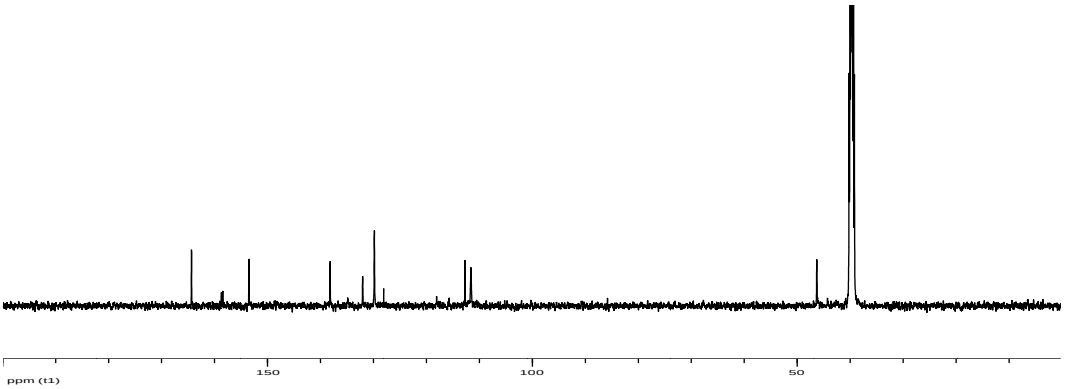

4-{[(6-{[(4-carbamimidoylphenyl)amino]methyl}pyridin-2-yl)methyl]amino}benzene-1-carboximidamide (10)

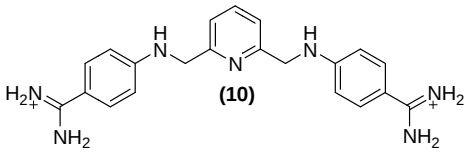

(10)

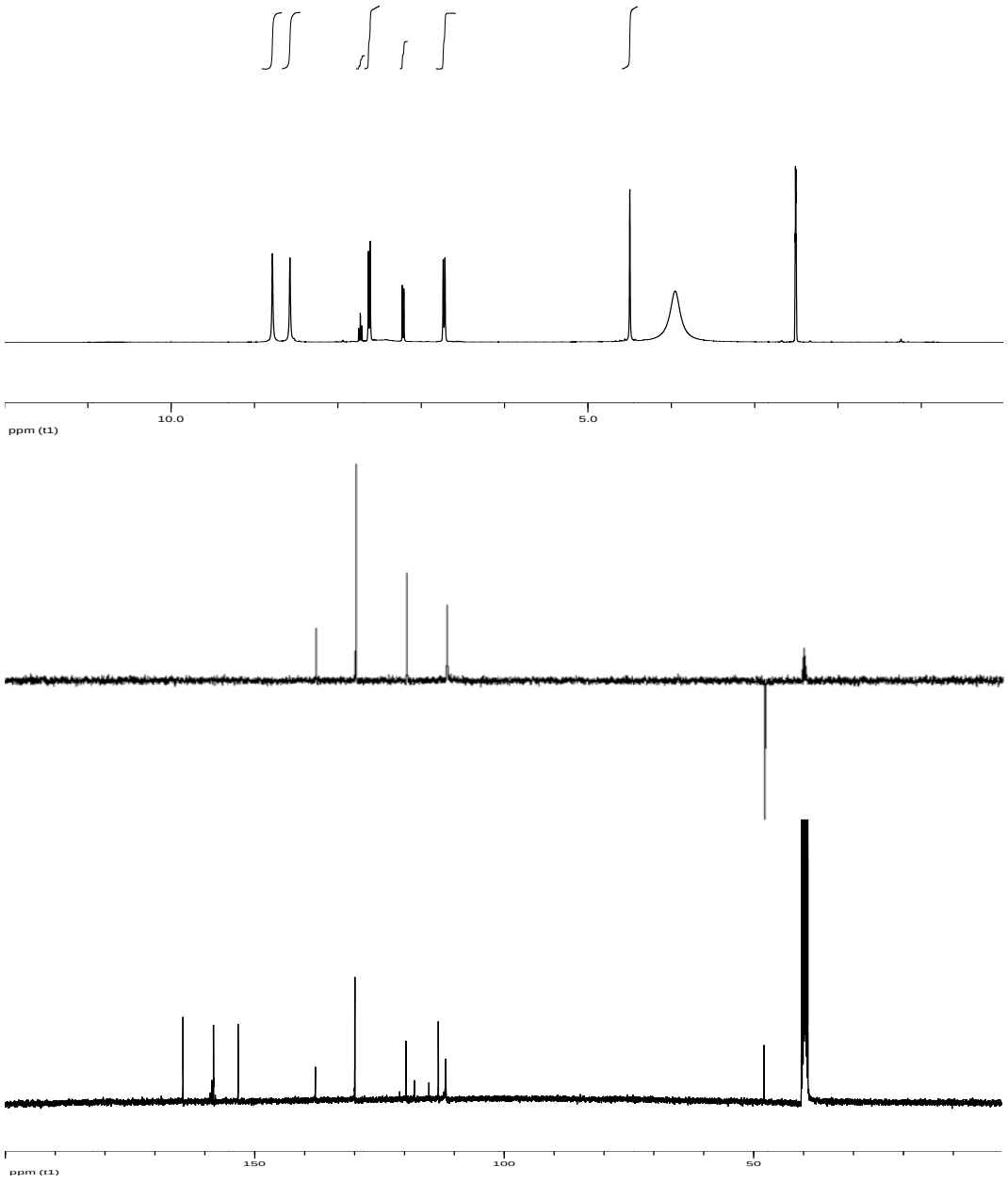

4-{[(3-{[(4-carbamimidoylphenyl)amino]methyl}-5-hydroxyphenyl)methyl]amino}benzene-1-carboximidamide (11)

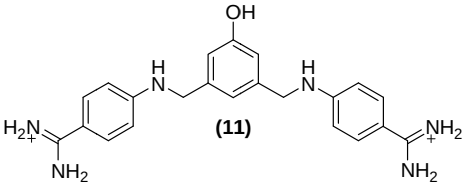

(11)

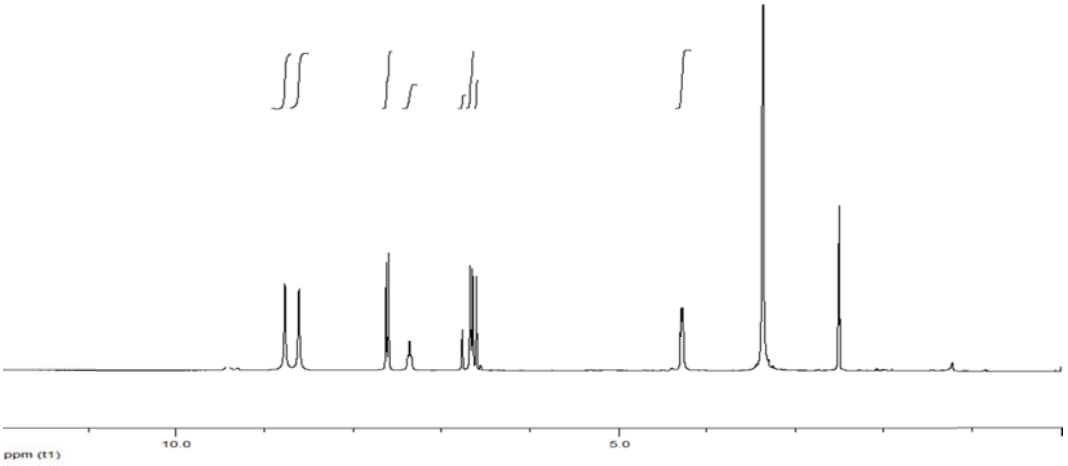

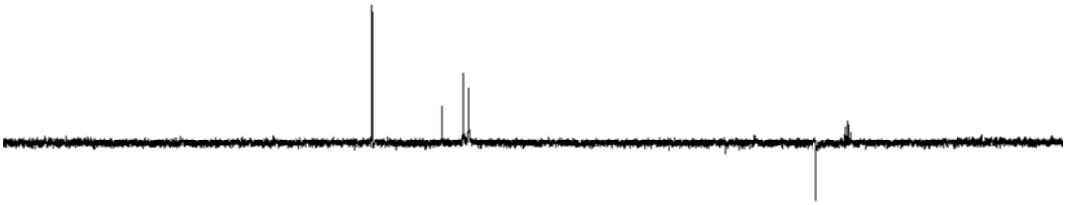

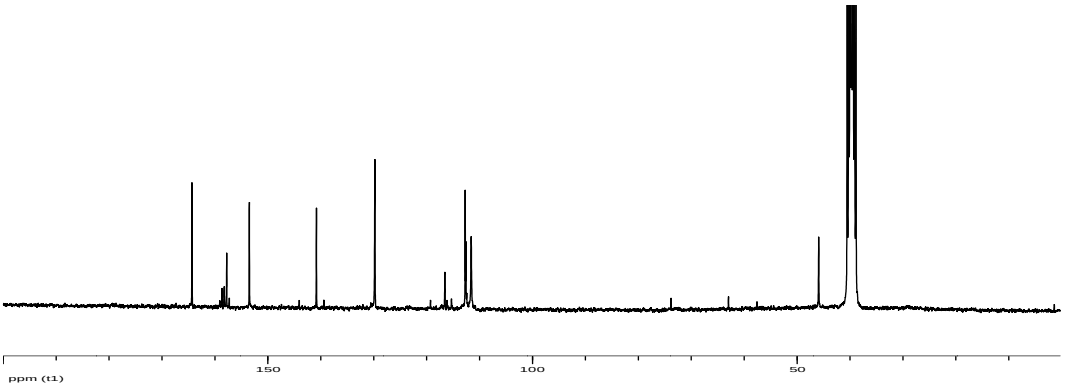

Furan-2,5-dicarbaldehyde (12a)

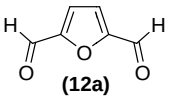

(12a)

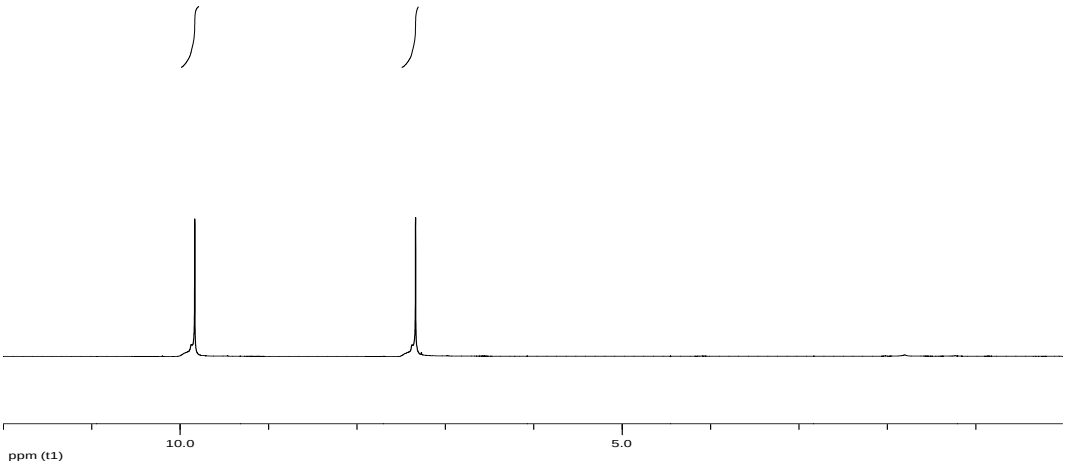

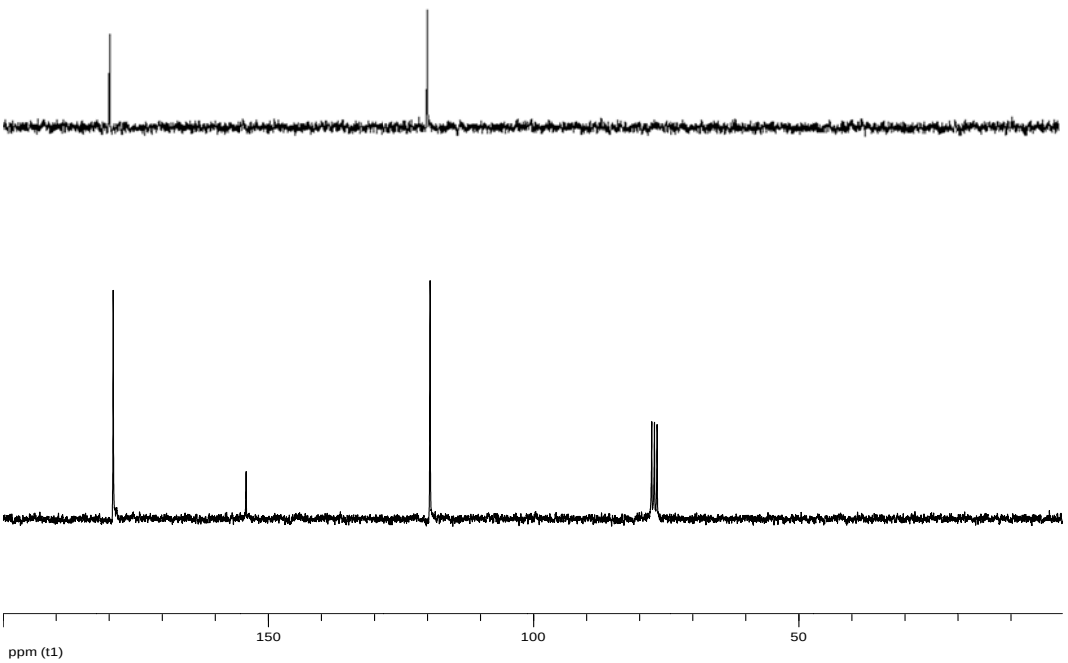

4-{[(5-{[(4-carbamimidoylphenyl)amino]methyl}furan-2-yl)methyl]amino}benzene-1-carboximidamide (12)

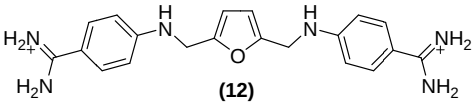

(12)

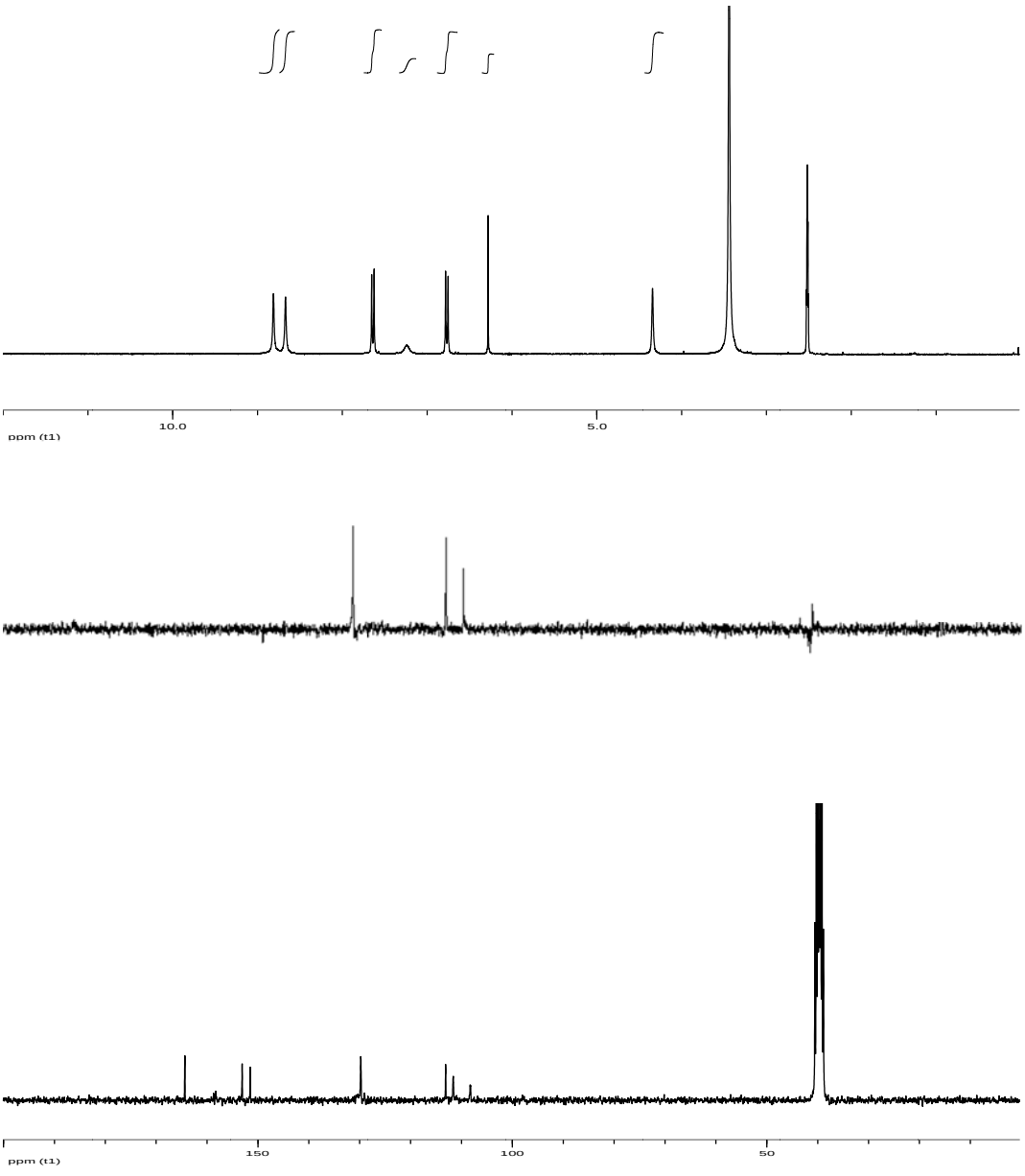

1-[3,5-bis({[(4-carbamimidoylphenyl)amino]methyl})phenyl]triaza-1,2-dien-2-ium (13)

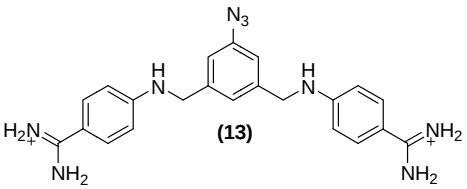

(13)

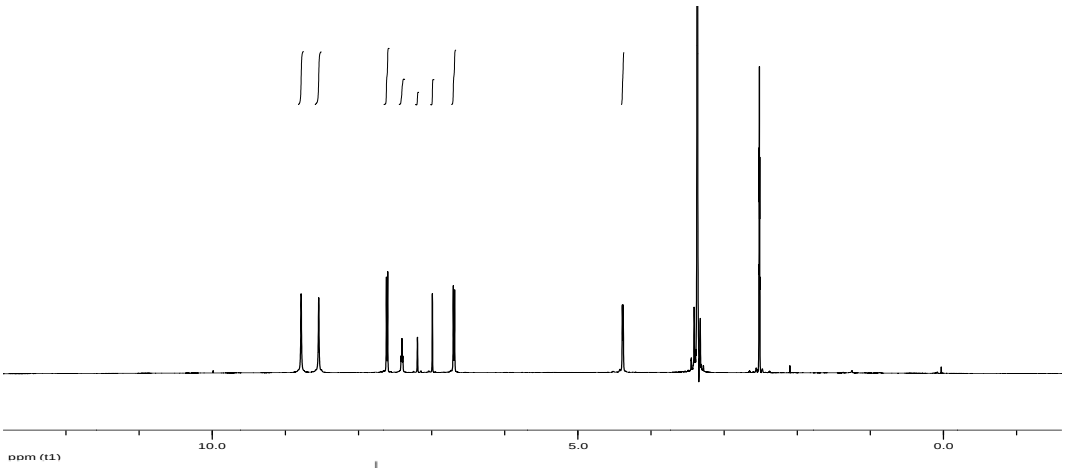

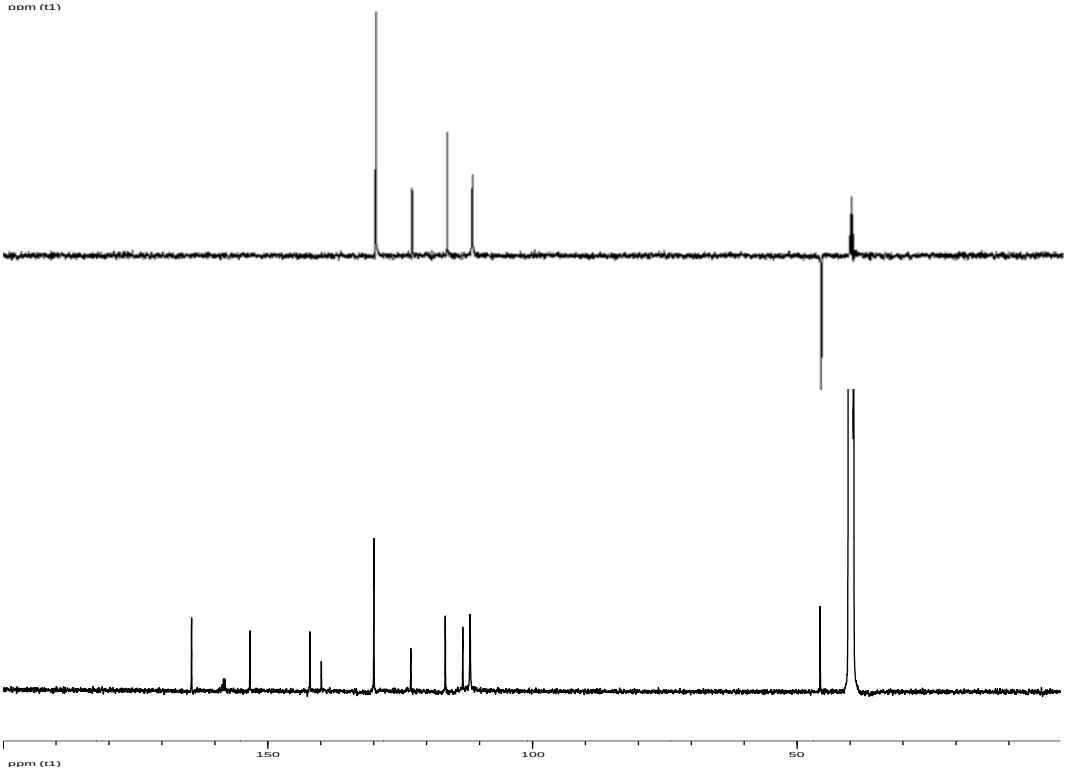

Prop-2-yn-1-yl 7-(diethylamino)-2oxo-2H-chromene-3-carboxylate (14a)

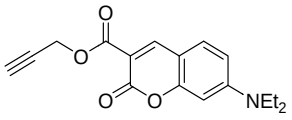

(14a)

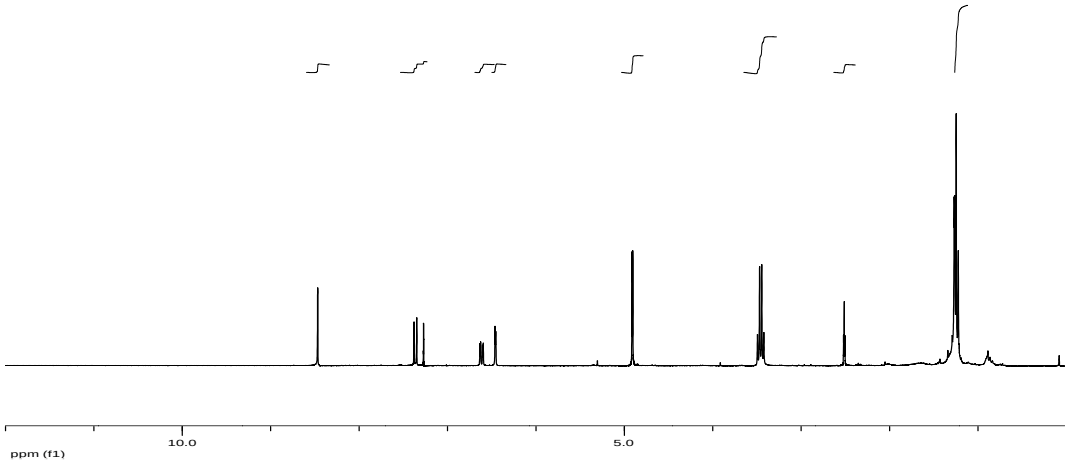

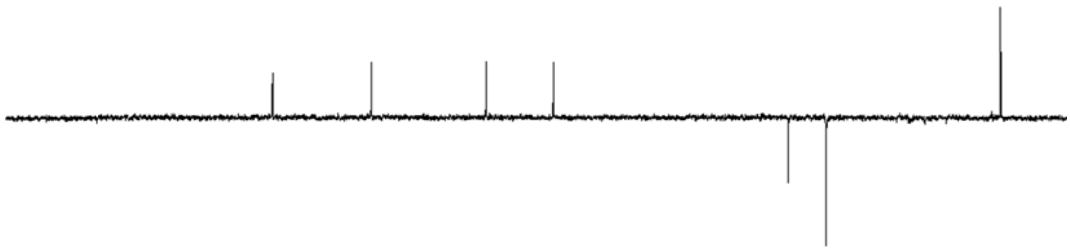

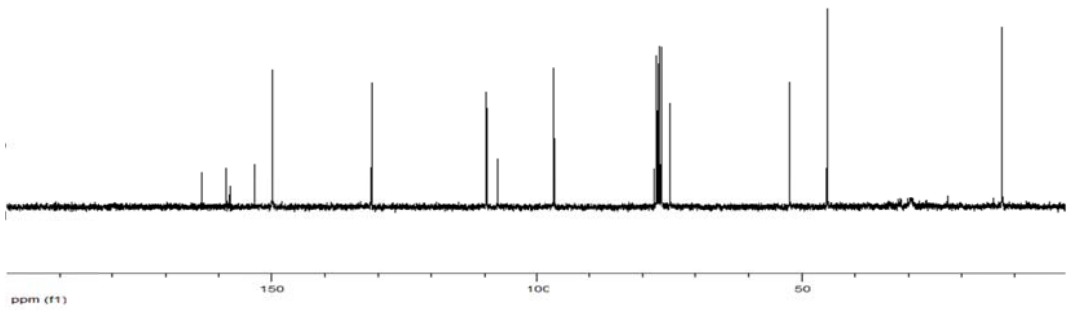

1-[3,5-bis({[(4-carbamimidoylphenyl)amino]methyl})phenyl]-1H-1,2,3-triazol-4-yl 7-(diethylamino)-2-oxo-2H-chromene-3-carboxylate (15a)

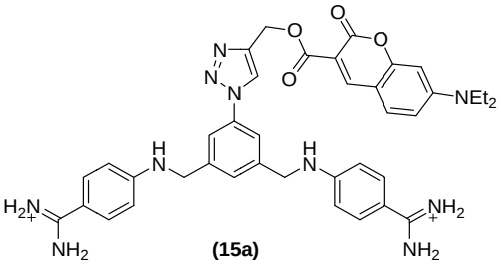

(15a)

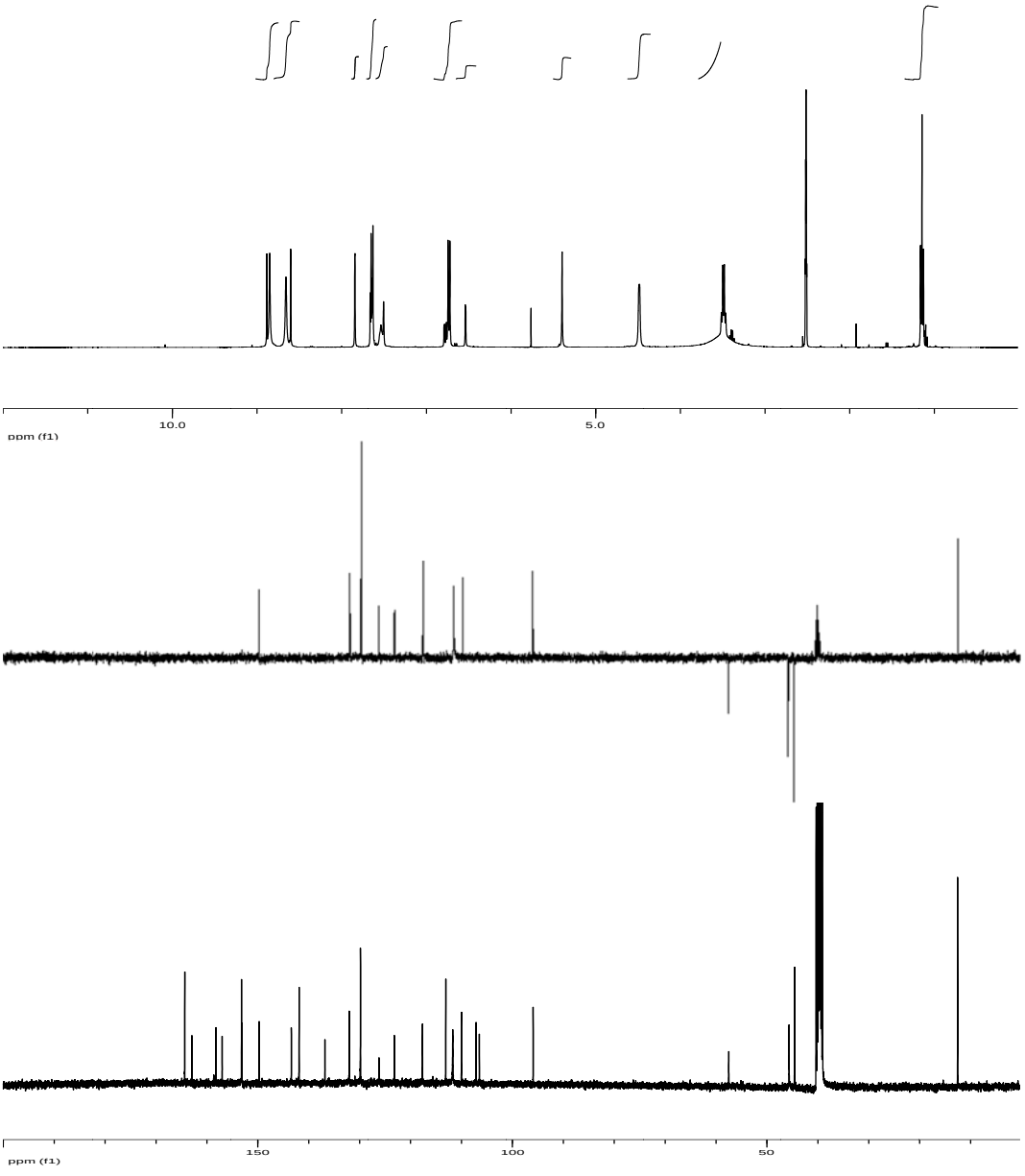

3-{1-[3,5-bis({[(4-carbamimidoylphenyl)amino]methyl})phenyl]-1H-1,2,3-triazol-4-yl}propanoic acid (16)

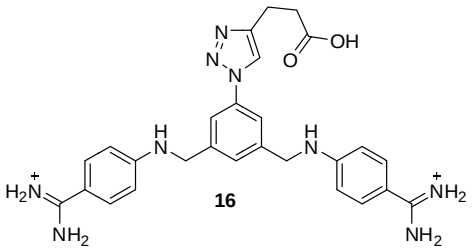

16

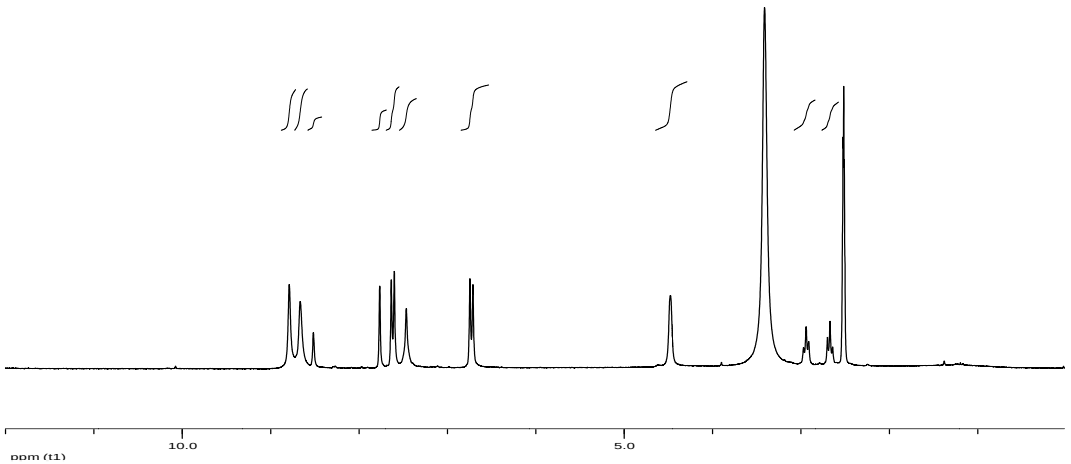

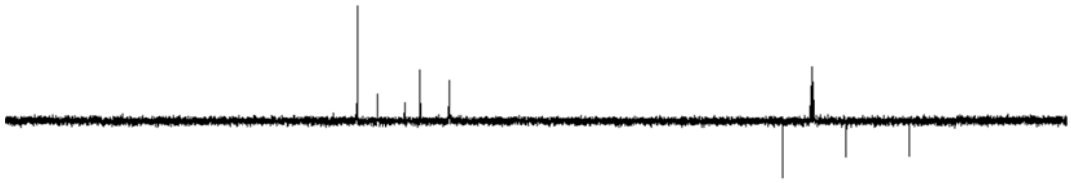

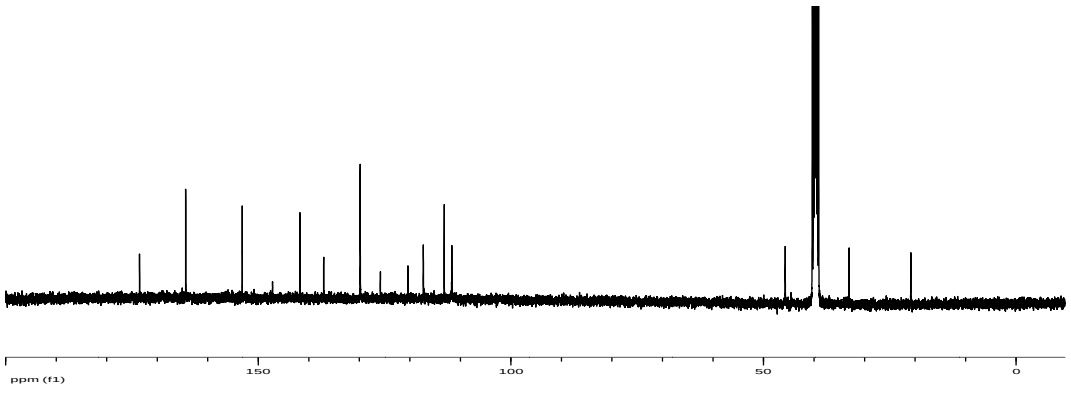

Peptide synthesis. All peptide synthesis reagents and amino acid derivatives were purchased from *GL Biochem* (Shanghai) and *Novabiochem*; amino acids were purchased as protected Fmoc amino acids with the standard side chain protecting scheme, except for the orthogonally protected Fmoc-Lys(Alloc)-OH and Fmoc-Ahx-OH, which were purchased from *Bachem*. Synthetic cJun was purchased from *Eurogentec*. C-terminal amide peptides were synthesized on a 0.1 mmol scale using a Fmoc-PAL-PEG-PS resin from *Applied Biosystems*. All solvents were dry and synthesis grade, unless specifically noted. Peptides were synthesized using an automatic *PS3* peptide synthesizer from *Protein Tecnologies* . Amino acids were coupled in 4-fold excess using HBTU/HOBt as activating agent. In the case of octaarginine, the amino acids were coupled using a 1:1 HATU/HOBt mixture as activating agent. Each amino acid was activated for 30 seconds in DMF before being added onto the resin. Peptide bond-forming couplings were conducted for 30 min to 45min. The deprotection of the temporal Fmoc protecting group was performed by treating the resin with 20% piperidine in DMF solution for 10 min. The final peptides were cleaved from the resin, and side-chain protecting groups were simultaneously removed using a standard TFA cleavage (50 μL of CH_2Cl_2, 25 μL of H_2O, 25 μL of TIS and 900 TFA μL for 40 mg of resin). High-Performance Liquid Chromatography (HPLC) was performed using an *Agilent 1100* series Liquid Chromatograph Mass Spectrometer system. Analytical HPLC was run using a *Zorbax Eclipse* XDB-C8 (5 μm) analytical column from Agilent. The purification of the peptides was performed on a *Jupiter Proteo* 90A (4 μm), reverse-phase column from *Phenomenex*. Amino acid sequences: cFos: MKRRIRRERNKMAAAKCRNRRRE LTDTLQAETDQLEDEKSALQTEIANLLKEKEKLW, cJun: FIKAERKRMRNRIAASKSRK RKLERIARLEEKVKTLKAQNSELASTANMLREQVAQLKQKVMNH.

Octaarginine-alkyne peptide 14b

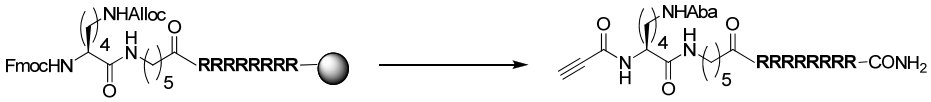

17 **14b**

Resin-bound peptide **17** was synthesized following standard peptide synthesis conditions. The selective deprotection of the lysine residue was carried out as following: approx. 6.7 μmol (25 mg of resin) of the peptide attached to the solid support were treated with PPh_3 (1.5 equiv), *N*-methyl morpholine (10 equiv) and phenylsilane (10 equiv) in CH_2Cl_2 (400 μL) at rt for 15 min. Subsequently $Pd(OAc)_2$ (0.3 equiv) was added and the resulting mixture was stirred overnight. The resin was filtered and washed with DMF (2 × 1.5 mL × 2 min), diethyl dithiocarbamate (DEDTC, 25 mg in 5 mL of DMF, 2 × 1.5 mL × 5 min), DMF (2 × 1.5 mL × 2 min) and CH_2Cl_2 (2 × 5 mL × 2 min).

The coupling of *p*-acetamidobenzoic acid was performed immediately after of the deprotection of the Lys(Alloc) residue, following standard conditions for amino acid couplings. Once the coupling was complete, according to the TNBS test on a small resin aliquot, the resin was filtered off and washed with DMF (2 × 1.5 mL × 2 min) and its terminal Fmoc group was removed following standard piperidine treatment. Propionic acid (8 equiv) was activated with HATU (8 equiv) and DIEA/DMF 0.2 M (8 equiv) and added to the resin. The reaction mixture was shaken for 2 h and the resin washed with DMF (2 × 1.5 mL × 2 min). The cleavage deprotection step was carried out under standard conditions (50 μL of CH_2Cl_2, 25 μL of H_2O, 25 μL of TIS and 900 TFA μL for 40 mg of resin) and the resulting crude purified by RP-HPLC obtaining the desired peptide (3.0 mg, 1.74 □mol, overall yield ≈ 25%)

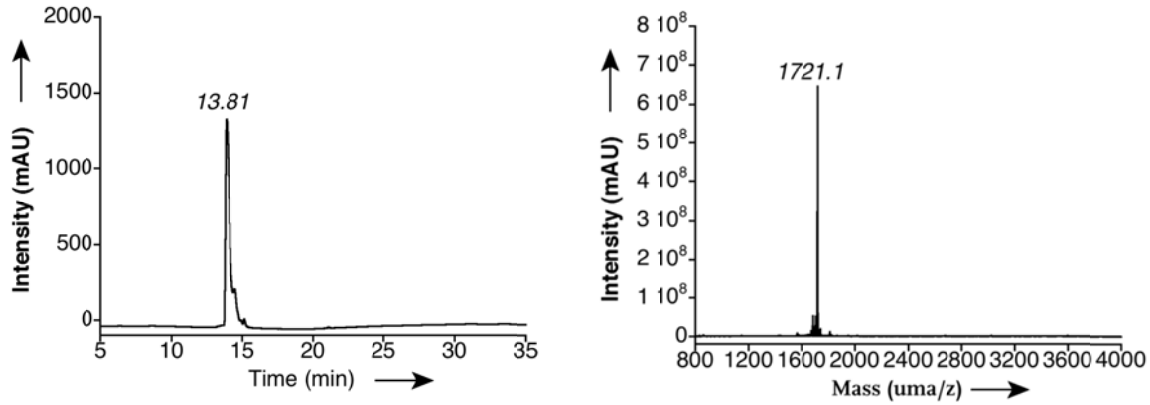

Figure S1. ***Left:*** *HPLC chromatogram of the peptide* ***14b*** *at 222 nm (gradient: 25% → 95%* water/methanol, 0.1% TFA*; flow: 1mL/min for 30 min).* ***Right:*** *MALDI of the peptide* ***14b****.*

Peptide **14b** : Exact mass calc. For: $C_{72}H_{129}N_{37}O_{13}$ 1720.0571, found 1721.1

Fos-alkyne peptide 14c

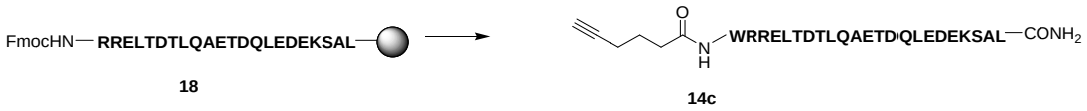

The Fmoc peptide was synthesized following standard conditions (aprox. 6.7 μmol of the peptide, 25 mg of resin), except for the final coupling of 4-pentynoic acid (10 equiv) which was accomplished after activation for 2 min with HATU (10 equiv) and DIEA/DMF 0.2 M. The reaction mixture was shaken for 2 h and the resin washed with DMF (2 × 1.5 mL × 2 min). Cleavage (50 μL of CH_2Cl_2, 25 μL of H_2O, 25 μL of TIS and 900 TFA μL for 40 mg of resin) and HPLC purification gave the desired product (4.45 mg, 1.47 μmol, overall yield ≈ 22%)

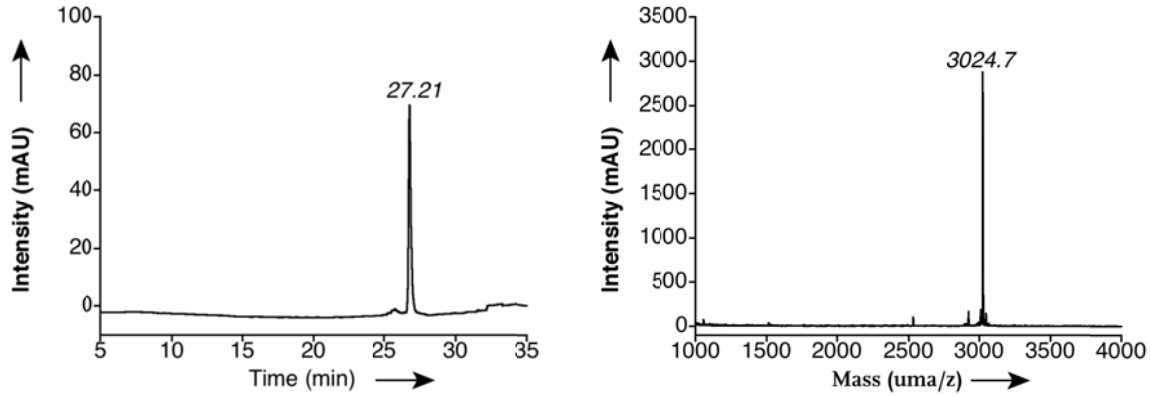

Figure S2. ***Left:*** *HPLC chromatogram of the peptide* ***14c*** *at 222 nm (gradient: 25% → 95%* water/methanol, 0.1% TFA*; flow: 1mL/min for 30 min).* ***Right:*** *MALDI of the peptide* ***14c****.*

Peptide **14c** :Exact mass calc. For: $C_{137}H_{200}N_{34}O_{44}$ 3025.4458 found 3024.7

#

General procedure for the click reaction of azide 13 and peptides 14b and 14c.

Synthesis of conjugate 15b

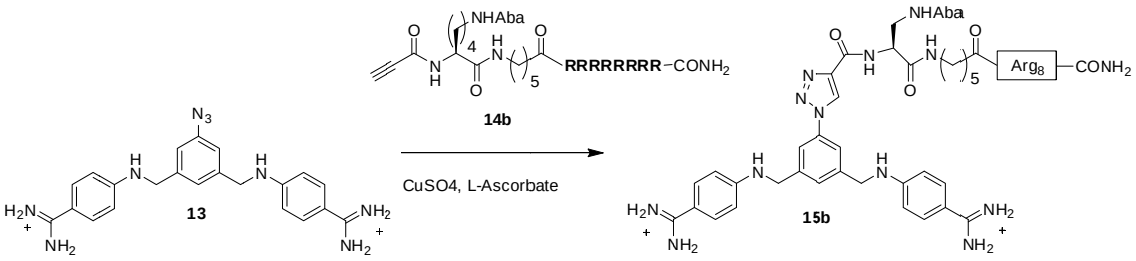

The alkyne functionalized peptide **14b** (0.001 mmol, 1.732 mg) and the azide derivative **13** (0.003 mmol, 1.92 mg) were dissolved in 100 μL of a buffer solution (20 mm Tris-HCl pH 7.5, 90 mm KCl, and 1.8 mm $MgCl_2$) so that the final concentration is approximately 100 μM for the alkyne. $CuSO_4 \times 5H_2O$ (0.01 μmol of a 1mM solution in water) and a freshly prepared solution of sodium ascorbate (0.04 μmol of 10 mM solution in water) were then added. The mixture was stirred at room temperature. After 12h, a small portion of the reaction mixture was analyzed by RP–HPLC. The chromatogram showed complete conversion of **13** obtaining **15b** with an approximately quantitative yield. The product was purified by RP–HPLC and characterized by MALDI-TOF mass spectrometry.

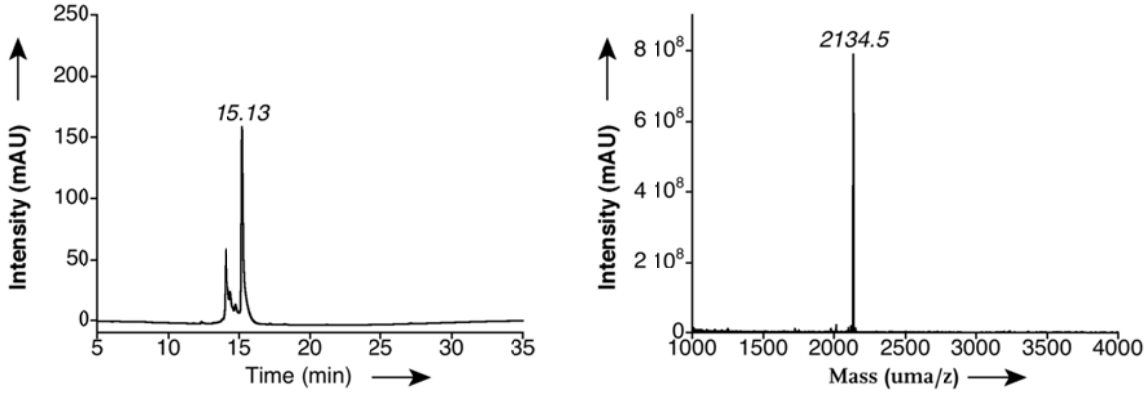

Figure S3. ***Left:*** *HPLC chromatogram of the click reaction between* ***13*** *and* ***14b*** *after 12h of reaction, showing the product (R.t. = 15.13) and excess of the alkyne functionalized peptide (R.t. = 13.81) (gradient: 5% → 95% water/ 0.1% TFA; flow: 1mL/min for 30 min, λ = 222 nm).* ***Right****: MALDI of the desired click product* ***15b****.*

Control experiments showed that in the absence of $CuSO_4$ no new product is observed when incubating the azide **13** with the alkyne **14b**. Addition of substoichiometric amounts (0.2 equiv) of the target dsDNA oligonucleotide did not promote the coupling; HPLC of the reaction residue showed only the starting materials.

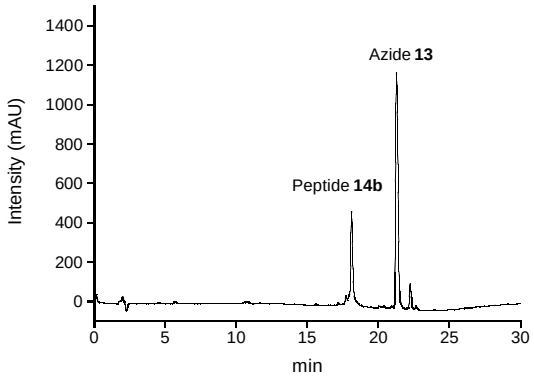

Figure S4. *HPLC trace of the mixture of peptide **14b** and azide **13** in the absence of $CuSO_4$ and in the presence of 0.2 equiv of target dsDNA* **A/T**:′-GAC *AAATTT* GAGAGTACGCT-*3′(gradient: 5 min 5%, 30 min 5 → 75% water / TFA 0.1%; flow: 1mL/min for 30 min, λ =: 304 nm). The DNA is not observed in the chromatogram, probably because of its low absorption at that detection wavelength. Note: we observed that addition of further amounts of dsDNA promotes precipitation.*

Synthesis of conjugate 15c

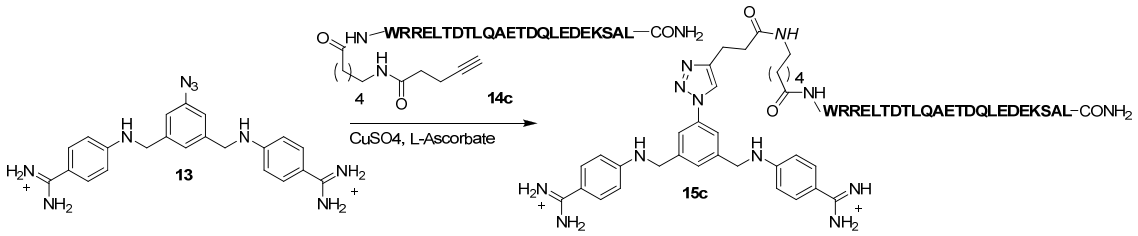

The alkyne functionalized peptide **14c** (0.001 mmol, 3.024 mg) and azide derivative **13** (0.003 mmol, 1.92 mg) were dissolved in 100 μL of a buffer solution (20 mm Tris-HCl pH 7.5, 90 mm KCl, and 1.8 mm $MgCl_2$) so that the final concentration is approximately 100 μM for the alkyne. $CuSO_4 \times 5H_2O$ (0.01 μmol of a 1mM solution in water) and freshly prepared solution of sodium ascorbate (0.04 μmol of 10 mM solution in water) were then added. The mixture was stirred at room temperature. After 12h, a small portion of the reaction mixture was analyzed by RP–HPLC, which showed complete conversion of **13** into **15c**. The product formed was purified by RP–HPLC and characterized by MALDI-TOF mass spectrometry

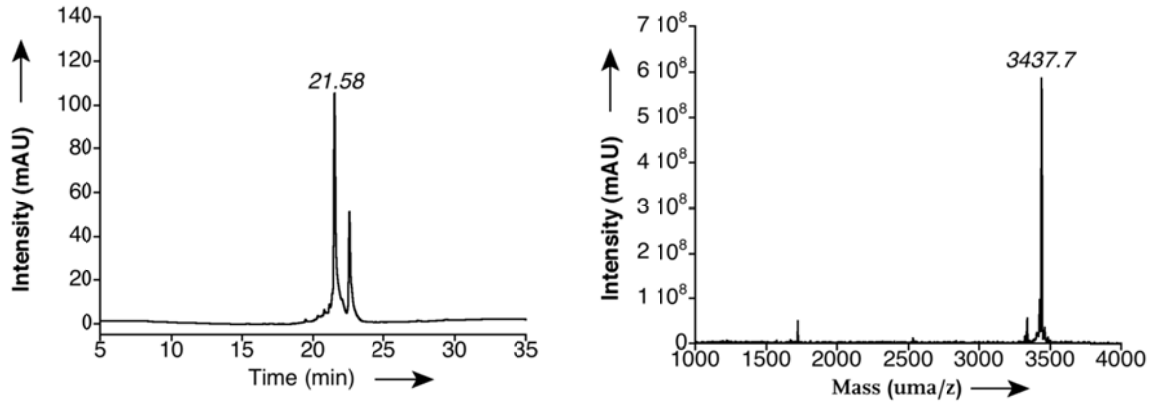

Figure S5. ***Left:*** *HPLC chromatogram of the click reaction for the preparation of peptide* ***15c****, after 12h of reaction, showing the product (R.t. = 21.58) and excess of the alkyne functionalized peptide (R.t. = 23.18) (gradient: 5% → 95% water/ 0.1% TFA; flow: 1mL/min for 30 min).* ***Right:*** *MALDI of the desired click product* ***15c****.*

Fluorescence titrations.

Measurements were made with a Jobin-Yvon *Fluoromax-3*, (DataMax 2.20) coupled to a Wavelength Electronics LFI−3751 temperature controller, using the following settings: increment: 1.0 nm; integration time: 0.2 s; excitation slit width: 3.0 nm; emission slit width: 6.0 nm; excitation wavelength 329 nm. The emission spectra were acquired from 345 to 500 nm at 20 ºC. All titrations were made following the same procedure: to 1 mL of a 0.5 μM solution of the select compound in Tris-HCl buffer 20 mM pH 7.5, 100 mM NaCl, aliquots of a ≈ 550 μM stock solution of the respective dsDNA were successively added, and the fluorescence spectra was recorded after each addition. Hairpin oligonucleotides were supplied by *Thermo Fischer* and their sequences were: **AAATTT**: 5'−GGC *AAATTT* CAG TTTTT CTG *AAATTT* GCC−3'; **AATTT**: 5'−GGCG *AATTT* CGC TTTTT GCG *AAATT* CGCC−3'; **AATT**: 5'−GGCG *AATT* CAGC TTTTT GCTG *AATT* CGCC−3'; **AAGTT**: 5'−GGCG *AAGTT* CGC TTTTT GCG *AACTT* CGCC−3'; **AGATT**: 5'−GGCG *AGATT* CGC TTTTT GCG *AATCT* CGCC−3'; **AAGCTT**: 5'−GGC *AAGCTT* CGC TTTTT GCG *AAGCTT* GCC−3'; **GGCCC**: 5'−GGCA *GGCC* CAGC TTTTT GCTG *GGCC* TGCC−3'.

Fitting to 1:1 binding modes was done as indicated in page S50.

Fluorescence titrations of azapentamidine (4) with different DNAs.

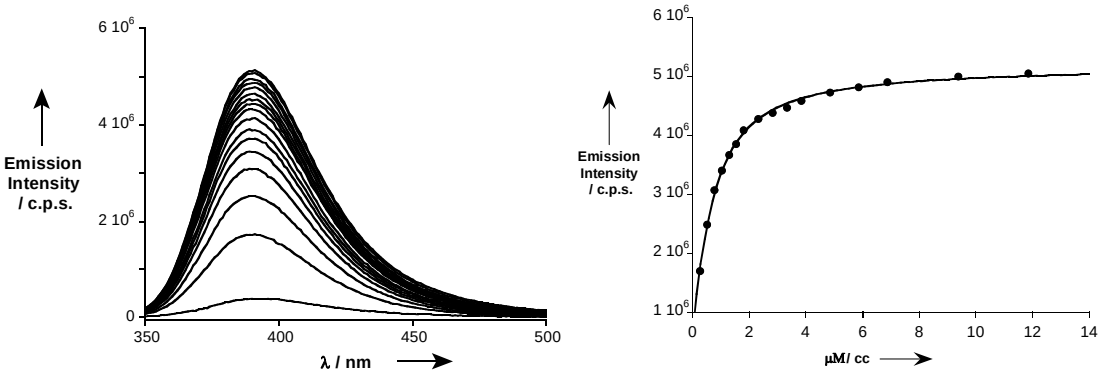

Figure S6. *Oligonucleotide* **AAATTT**. **Left**: fluorescence emission spectra of **4** in the presence of successive aliquots of target oligonucleotide. **Right:** Plot of the fluorescence emission at 386 nm against the total ds-DNA concentration and best-fit curve to a 1:1 binding mode. *Estimated K_D (average of three experiments): K_D= 393 ± 56 nM.*

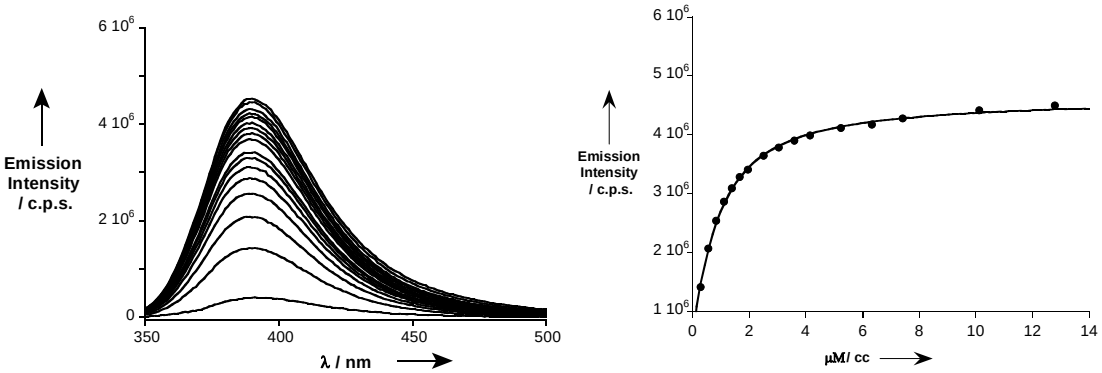

Figure S7. *Oligonucleotide* **AATTT**. **Left**: fluorescence emission spectra of **4** in the presence of successive aliquots of target oligonucleotides. **Right:** Plot of the fluorescence emission at 386 nm against the total ds-DNA concentration and best-fit curve to a 1:1 binding mode. *Estimated K_D (average of three experiments): K_D= 628 ± 77 nM.*

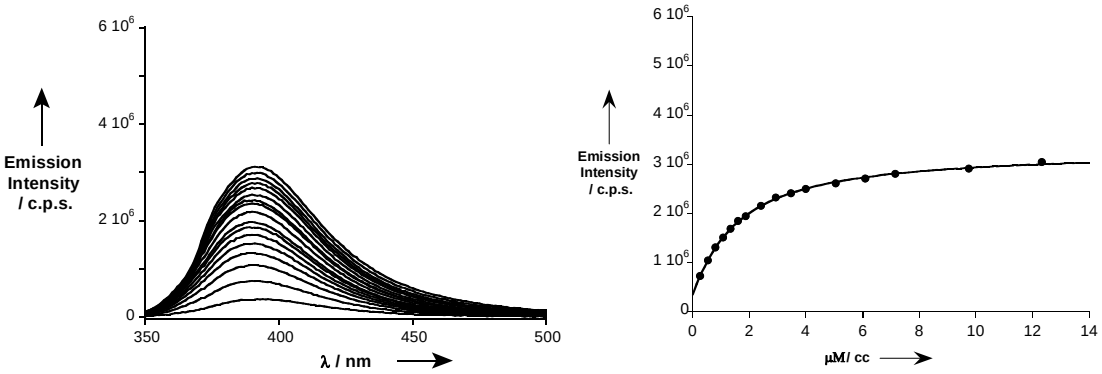

Figure S8. *Oligonucleotide* **AATT**. **Left**: fluorescence emission spectra of **4** in the presence of successive aliquots of target oligonucleotide. **Right:** Plot of the fluorescence emission at 386 nm against the total ds-DNA concentration and best-fit curve to a 1:1 binding mode. *Estimated K_D (average of three experiments): K_D= 1.1 ± 0.1 µM.*

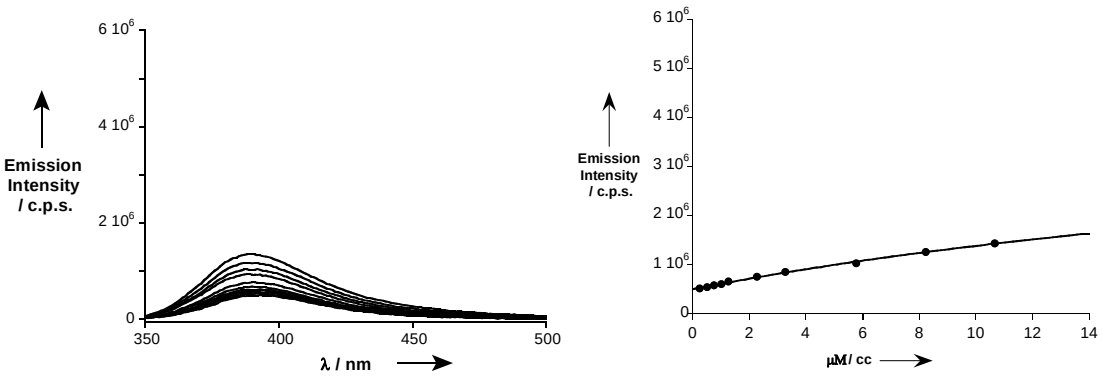

Figure S9. *Oligonucleotide* **GGCCC. Left**: fluorescence emission spectra of **4** in the presence of successive aliquots of target oligonucleotide. **Right:** Plot of the fluorescence emission at 386 nm against the total ds-DNA concentration.

Fluorescence titrations of m-phenyl derivative 7 with different DNAs.

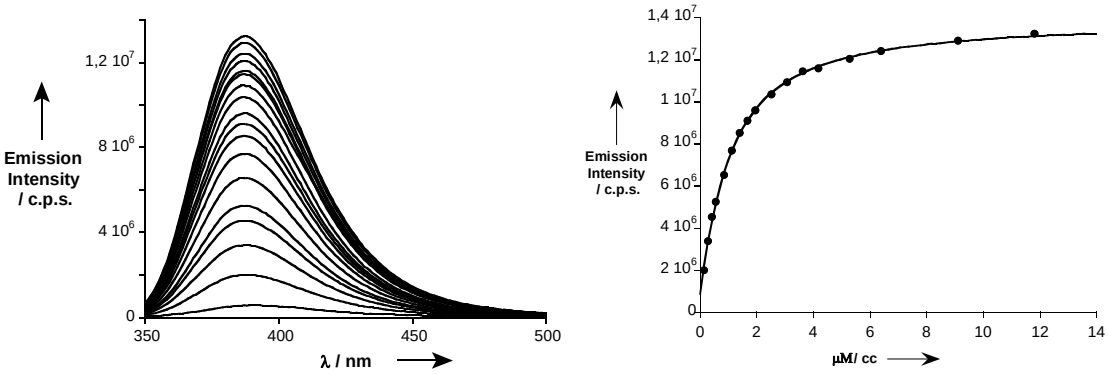

Figure S10. *Oligonucleotide* **AAATTT**. **Left**: fluorescence emission spectra of **7** in the presence of successive aliquots of target oligonucleotide. **Right:** Plot of the fluorescence emission at 386 nm against the total ds-DNA concentration and best-fit curve to a 1:1 binding mode. *Estimated K_D (average of three experiments): K_D= 724 ± 89 nM.*

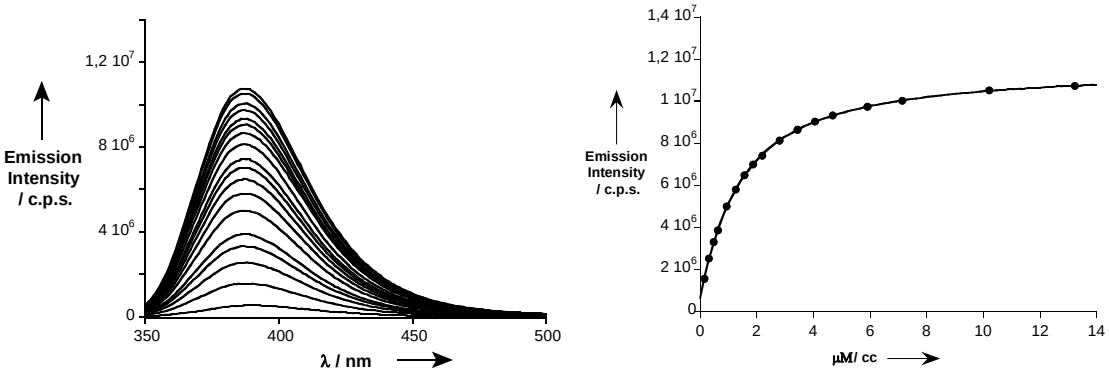

Figure S11. *Oligonucleotide* **AATTT**. **Left**: fluorescence emission spectra of **7** in the presence of successive aliquots of target oligonucleotide. **Right:** Plot of the fluorescence emission at 386 nm against the total ds-DNA concentration and best-fit curve to a 1:1 binding mode. *Estimated K_D (average of three experiments): K_D= 1.2 ± 0.1 µM.*

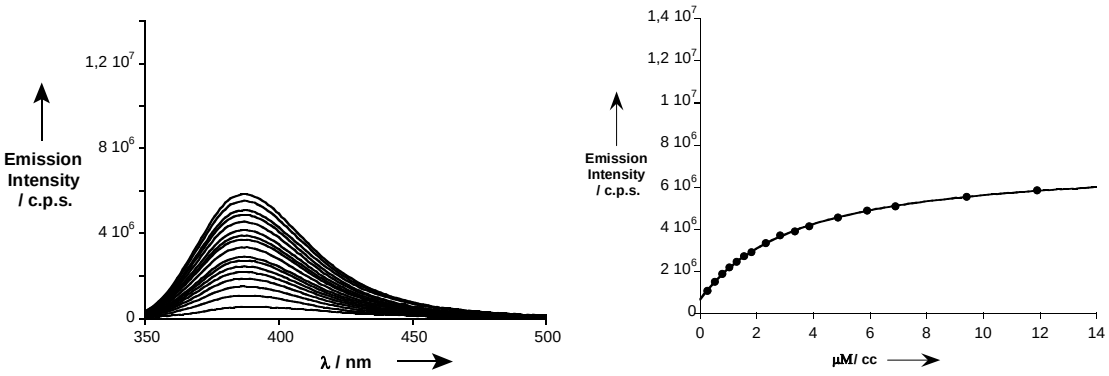

Figure S12. *Oligonucleotide* **AATT**. **Left**: fluorescence emission spectra of **7** in the presence of successive aliquots of target oligonucleotide. **Right:** Plot of the fluorescence emission at 386 nm against the total ds-DNA concentration and best-fit curve to a 1:1 binding mode. *Estimated K_D (average of three experiments): K_D= 1.8 ± 0.1 µM.*

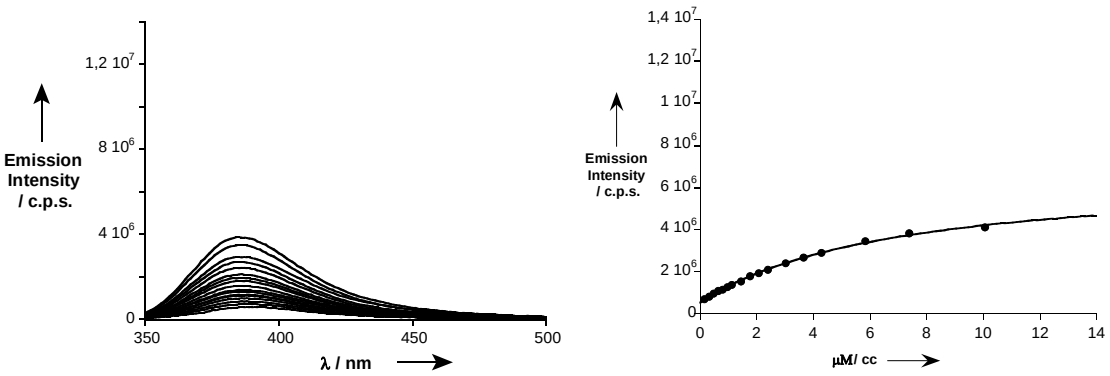

Figure S13. *Oligonucleotide* **AAGTT**. **Left**: fluorescence emission spectra of **7** in the presence of successive aliquots of target oligonucleotide. **Right:** Plot of the fluorescence emission at 386 nm against the total ds-DNA concentration and best-fit curve to a 1:1 binding mode. *Estimated K_D (average of three experiments): K_D= 9.1 ± 2.8 μM.*

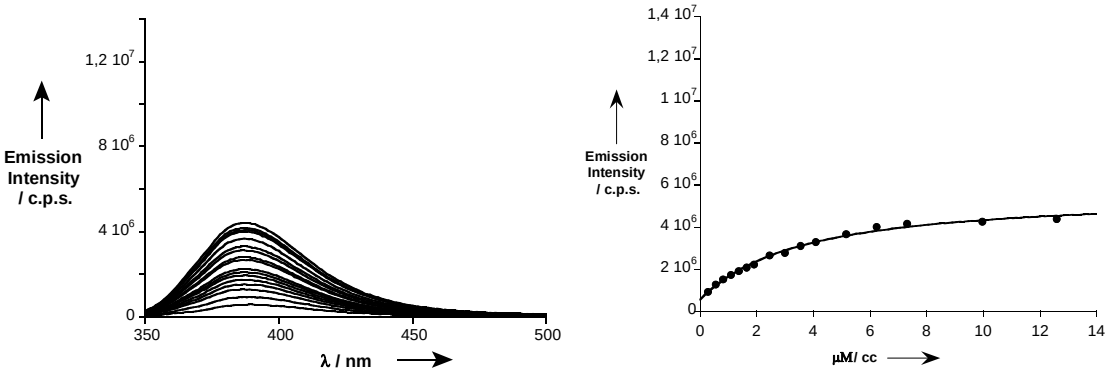

Figure S14. *Oligonucleotide* **AGATT**. **Left**: fluorescence emission spectra of **7** in the presence of successive aliquots of target oligonucleotides. **Right:** Plot of the fluorescence emission at 386 nm against the total ds-DNA concentration and best-fit curve to a 1:1 binding mode. *Estimated K_D (average of three experiments): K_D= 10.2 ± 2.2 μM.*

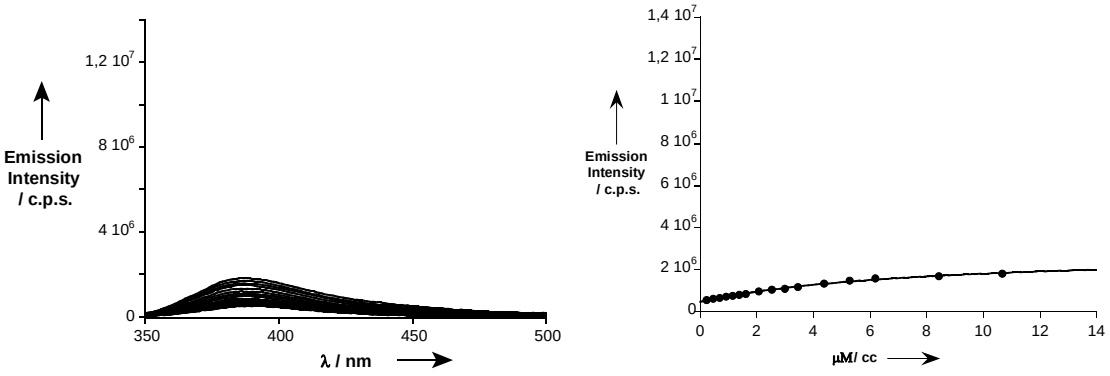

Figure S15. *Oligonucleotide* **AAGCTT**. **Left**: fluorescence emission spectra of **7** in the presence of successive aliquots of target oligonucleotide. **Right:** Plot of the fluorescence emission at 386 nm against the total ds-DNA concentration. *Estimated K_D > 15 μM.*

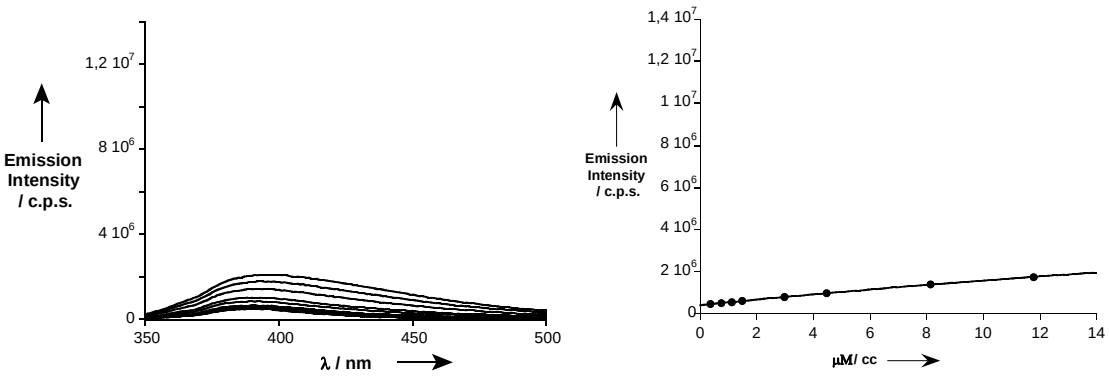

Figure S16. *Oligonucleotide* **GGCCC**. **Left**: fluorescence emission spectra of **7** in the presence of successive aliquots of target oligonucleotide. **Right:** Plot of the fluorescence emission at 386 nm against the total ds-DNA concentration.

Fluorescence titrations of p-phenyl derivative 8 with different DNAs.

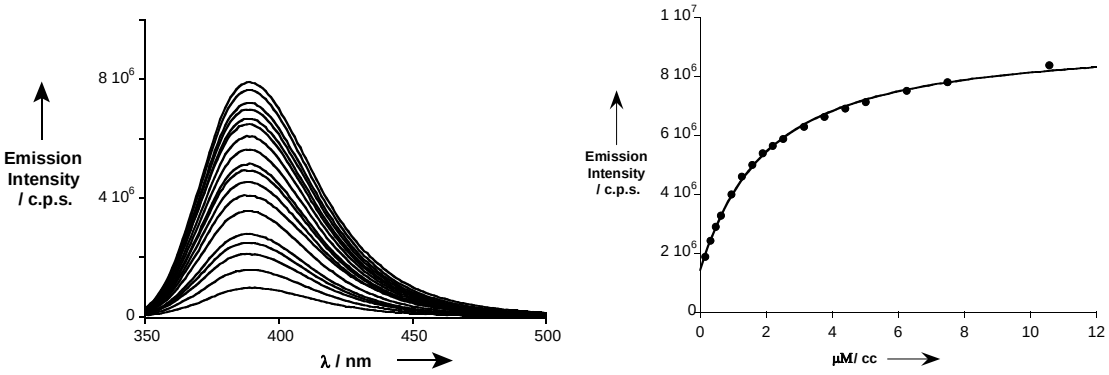

Figure S17. *Oligonucleotide* **AAATTT**. **Left**: fluorescence emission spectra of **8** in the presence of successive aliquots of target oligonucleotide. **Right:** Plot of the fluorescence emission at 386 nm against the total ds-DNA concentration and best-fit curve to a 1:1 binding mode. *Estimated K_D value (average of three experiments): K_D= 1.3 ± 0.2 μM.*

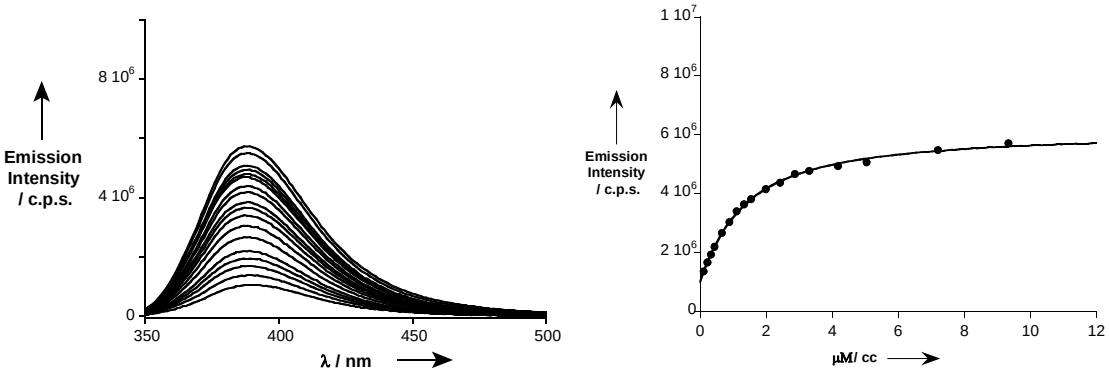

Figure S18. *Oligonucleotide* **AATTT**. **Left**: fluorescence emission spectra of **8** in the presence of successive aliquots of target oligonucleotides. **Right:** Plot of the fluorescence emission at 386 nm against the total ds-DNA concentration and best-fit curve to a 1:1 binding mode. *Estimated K_D value (average of three experiments): K_D= 1.5 ± 0.2 μM.*

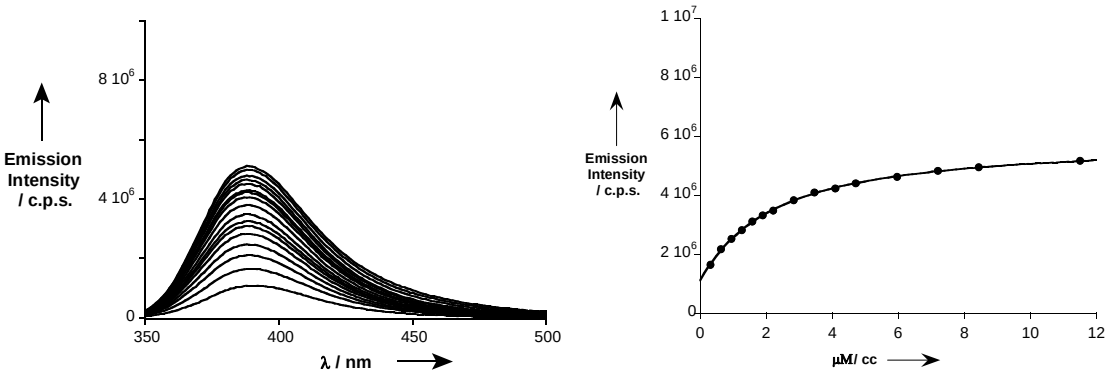

Figure S19. *Oligonucleotide* **AATT**. **Left**: fluorescence emission spectra of **8** in the presence of successive aliquots of target oligonucleotide. **Right:** Plot of the fluorescence emission at 386 nm against the total ds-DNA concentration and best-fit curve to a 1:1 binding mode. *Estimated K_D value (average of three experiments): K_D= 1.7 ± 0.1 μM.*

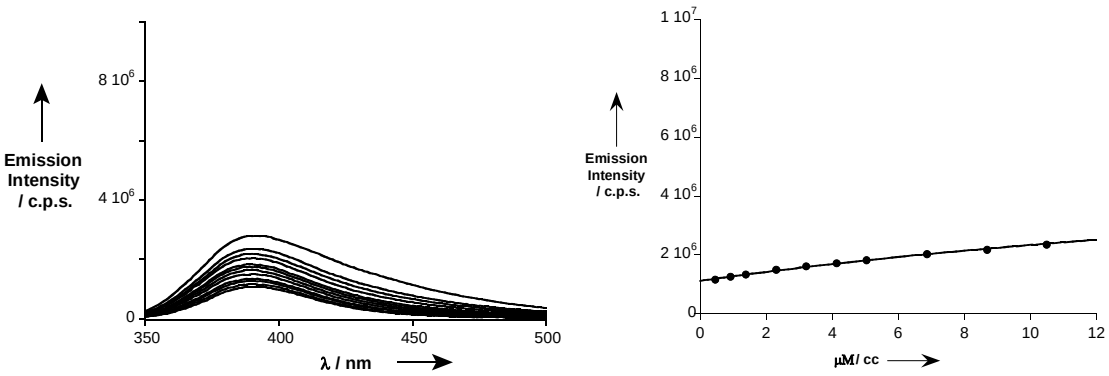

Figure S20. *Oligonucleotide* **GGCCC**. **Left**: fluorescence emission spectra of **8** in the presence of successive aliquots of target oligonucleotides. **Right:** Plot of the fluorescence emission at 386 nm against the total ds-DNA concentration .

Fluorescence titrations of boronic acid derivative 9 with different DNAs.

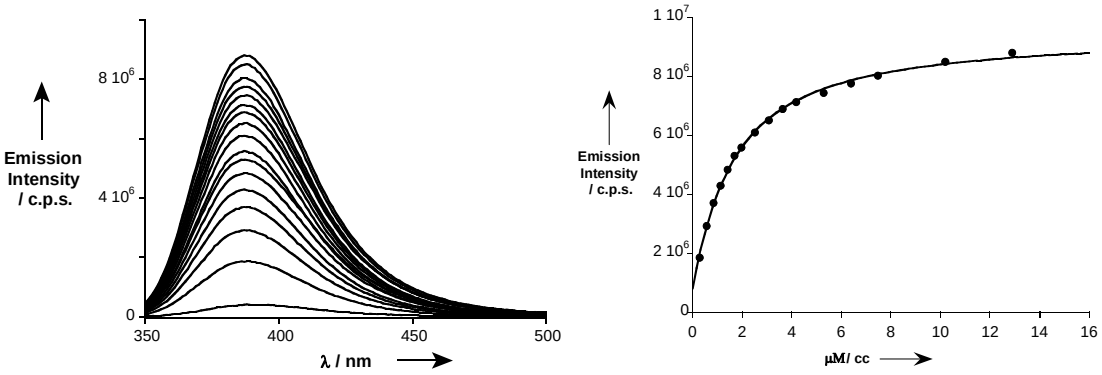

Figure S21. *Oligonucleotide* **AAATTT**. **Left**: fluorescence emission spectra of **9** in the presence of successive aliquots of target oligonucleotide. **Right:** Plot of the fluorescence emission at 386 nm against the total ds-DNA concentration and best-fit curve to a 1:1 binding mode. *Estimated K_D (average of three experiments): K_D= 1.1 ± 0.1 µM.*

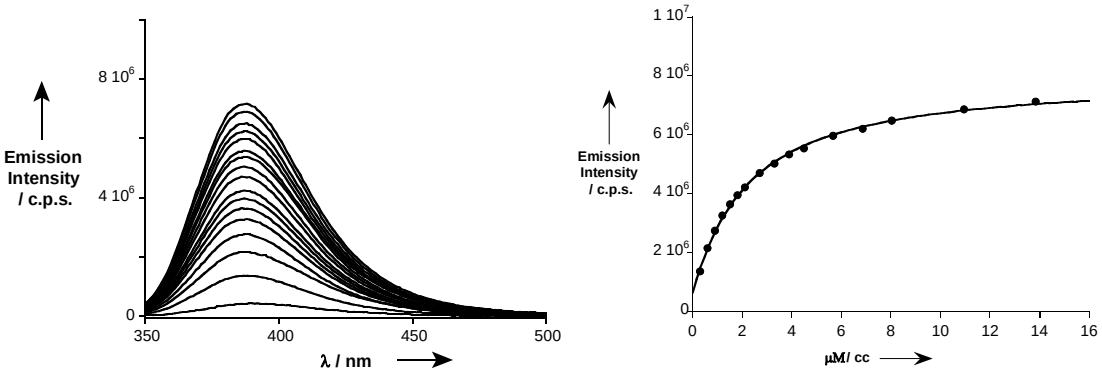

Figure S22. *Oligonucleotide* **AATTT**. **Left**: fluorescence emission spectra of **9** in the presence of successive aliquots of target oligonucleotide. **Right:** Plot of the fluorescence emission at 386 nm against the total ds-DNA concentration and best-fit curve to a 1:1 binding mode. *Estimated K_D (average of three experiments): K_D= 1.5 ± 0.2 µM.*

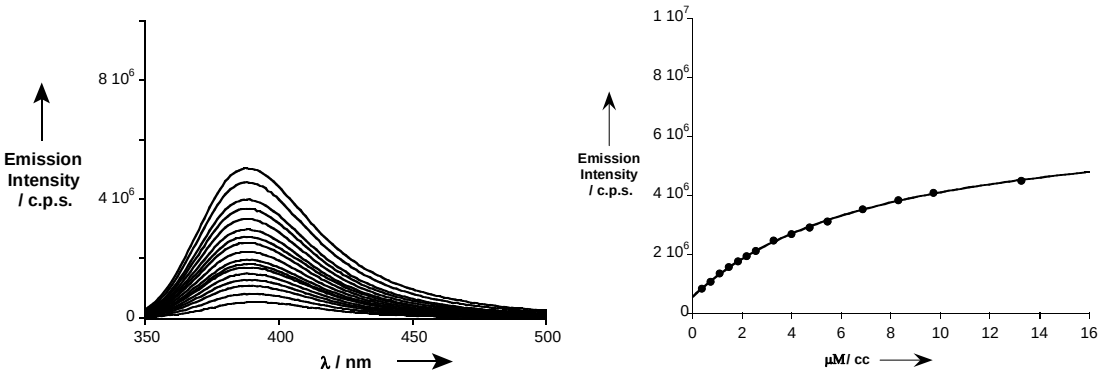

Figure S23. *Oligonucleotide* **AATT**. **Left**: fluorescence emission spectra of **9** in the presence of successive aliquots of target oligonucleotide. **Right:** Plot of the fluorescence emission at 386 nm against the total ds-DNA concentration and best-fit curve to a 1:1 binding mode. *Estimated K_D (average of three experiments): K_D= 3.2 ± 0.5 µM.*

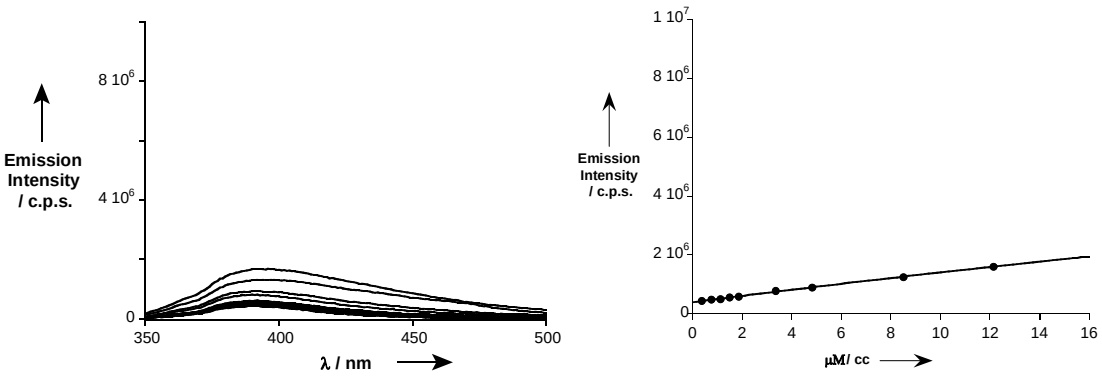

Figure S24. *Oligonucleotide* **GGCCC. Left**: fluorescence emission spectra of **9** in the presence of successive aliquots of target oligonucleotide. **Right:** Plot of the fluorescence emission at 386 nm against the total ds-DNA concentration.

Fluorescence titrations of pyridine derivative 10 with different DNAs.

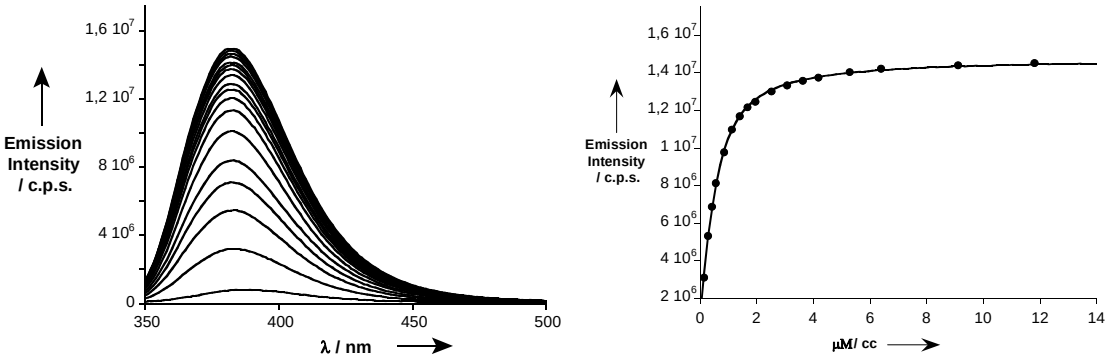

Figure S25. *Oligonucleotide* **AAATTT**. **Left**: fluorescence emission spectra of **10** in the presence of successive aliquots of target oligonucleotide. **Right:** Plot of the fluorescence emission at 386 nm against the total ds-DNA concentration and best-fit curve to a 1:1 binding mode. *Estimated K_D (average of three experiments): K_D= 229 ± 63 nM.*

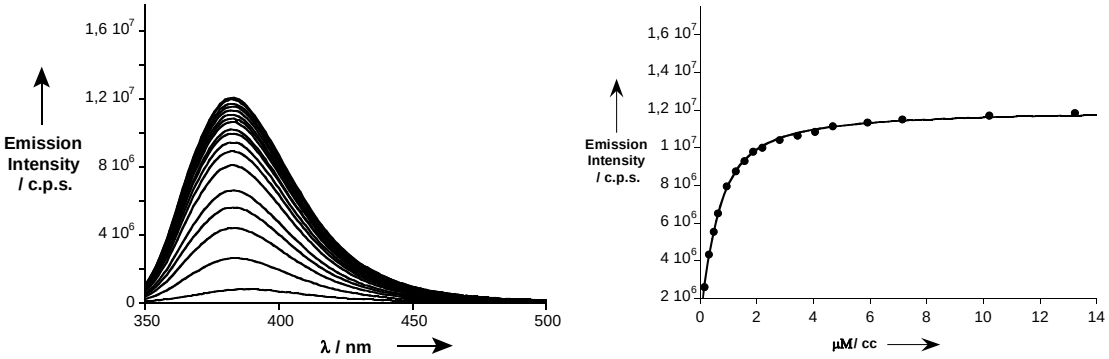

Figure S26. *Oligonucleotide* **AATTT**. **Left**: fluorescence emission spectra of **10** in the presence of successive aliquots of target oligonucleotides. **Right:** Plot of the fluorescence emission at 386 nm against the total ds-DNA concentration and best-fit curve to a 1:1 binding mode. *Estimated K_D (average of three experiments): K_D= 334 ± 40 nM.*

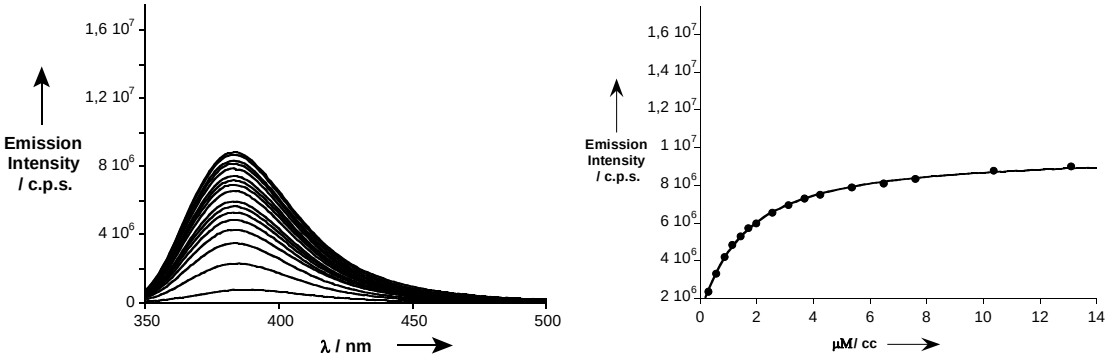

Figure S27. *Oligonucleotide* **AATT**. **Left**: fluorescence emission spectra of **10** in the presence of successive aliquots of target oligonucleotide. **Right:** Plot of the fluorescence emission at 386 nm against the total ds-DNA concentration and best-fit curve to a 1:1 binding mode. *Estimated K_D (average of three experiments): K_D= 1.0 ± 0.2 μM.*

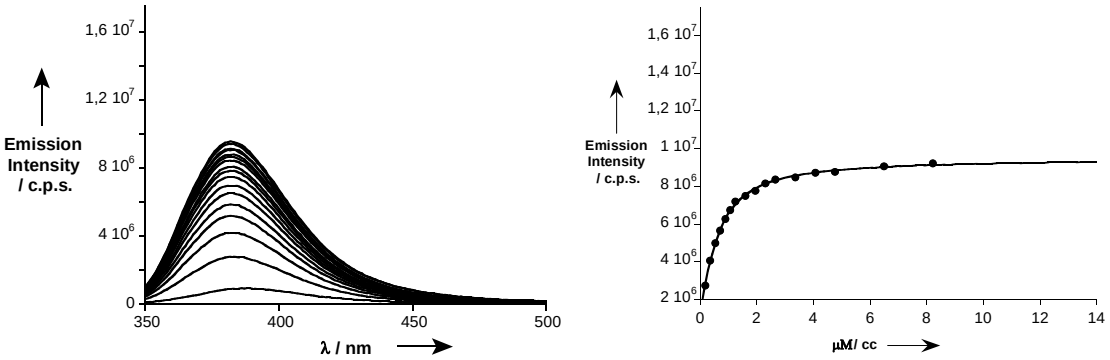

Figure S28. *Oligonucleotide* **AAGTT**. **Left**: fluorescence emission spectra of **10** in the presence of successive aliquots of target oligonucleotide. **Right:** Plot of the fluorescence emission at 386 nm against the total ds-DNA concentration and best-fit curve to a 1:1 binding mode. *Estimated K_D (average of three experiments): K_D= 396 ± 72 nM.*

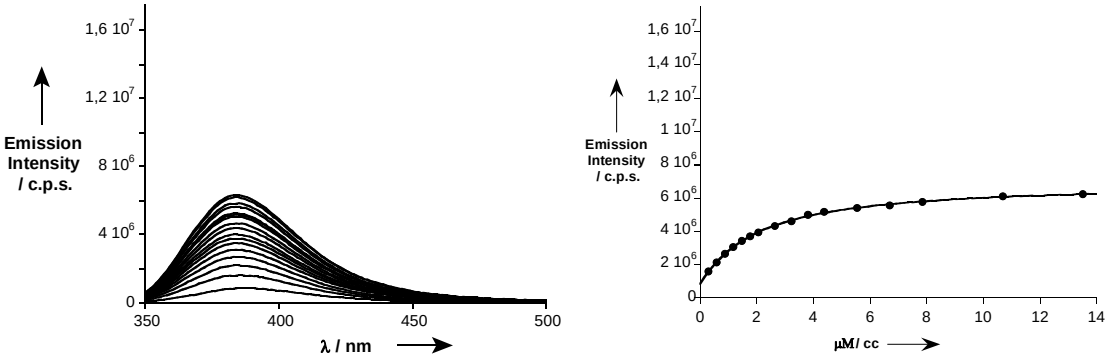

Figure S29. *Oligonucleotide* **AGATT**. **Left**: fluorescence emission spectra of **10** in the presence of successive aliquots of target oligonucleotide. **Right:** Plot of the fluorescence emission at 386 nm against the total ds-DNA concentration and best-fit curve to a 1:1 binding mode. *Estimated K_D (average of three experiments): K_D= 1.9 ± 0.1 µM.*

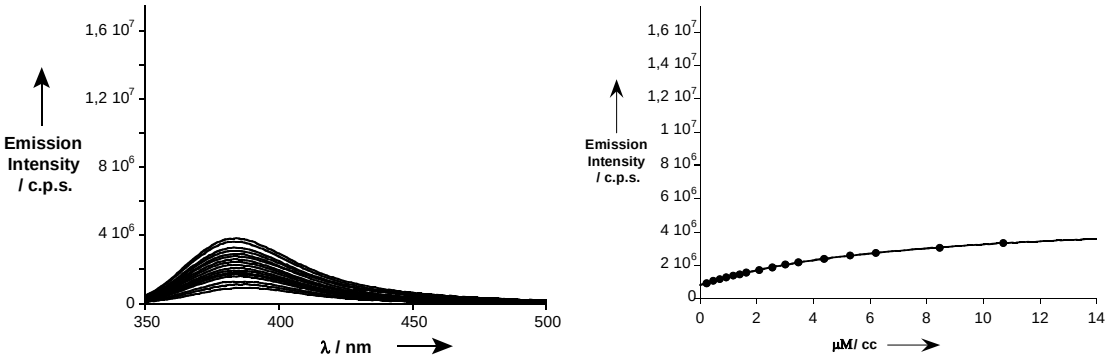

Figure S30. *Oligonucleotide* **AAGCTT**. **Left**: fluorescence emission spectra of **10** in the presence of successive aliquots of target oligonucleotide. **Right:** Plot of the fluorescence emission at 386 nm against the total ds-DNA concentration and best-fit curve to a 1:1 binding mode. *Estimated K_D (average of three experiments): K_D= 6.3 ± 0.8 µM.*

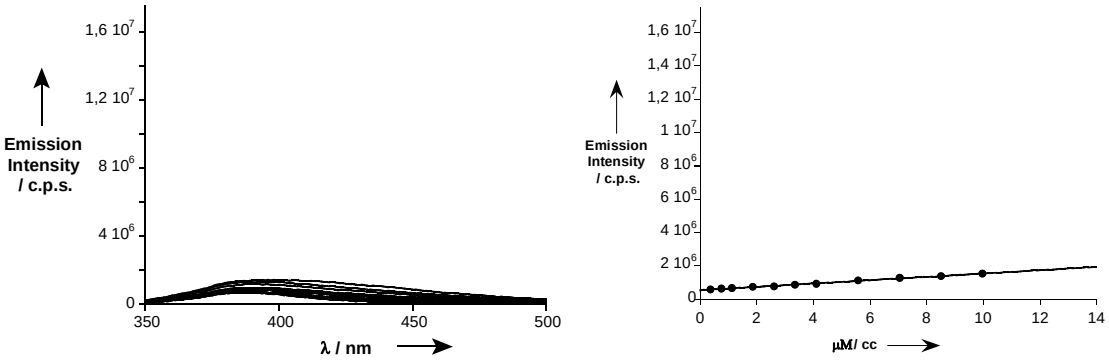

Figure S31. *Oligonucleotide* **GGCCC**. **Left**: fluorescence emission spectra of **10** in the presence of successive aliquots of target oligonucleotides. **Right:** Plot of the fluorescence emission at 386 nm against the total ds-DNA concentration.

Fluorescence titrations of phenol derivative 11 with different DNAs.

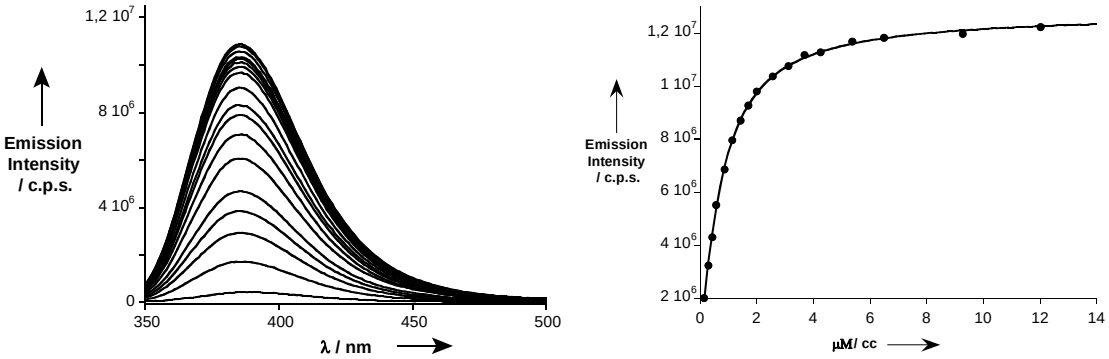

Figure S32. *Oligonucleotide* **AAATTT**. **Left**: fluorescence emission spectra of **11** in the presence of successive aliquots of target oligonucleotide. **Right:** Plot of the fluorescence emission at 386 nm against the total ds-DNA concentration and best-fit curve to a 1:1 binding mode. *Estimated K_D (average of three experiments): K_D= 563 ± 55 nM.*

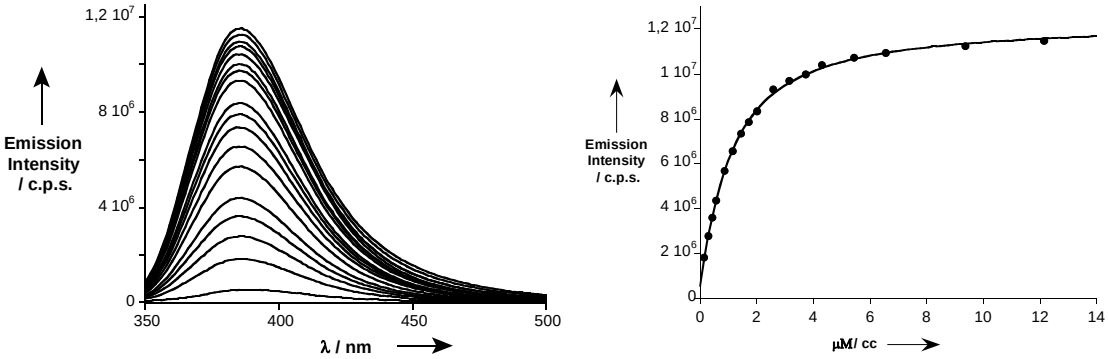

Figure S33. *Oligonucleotide **AATTT***. **Left**: fluorescence emission spectra of **11** in the presence of successive aliquots of target oligonucleotide. **Right:** Plot of the fluorescence emission at 386 nm against the total ds-DNA concentration and best-fit curve to a 1:1 binding mode. *Estimated K_D (average of three experiments): K_D= 1.0 ± 0.1 μM.*

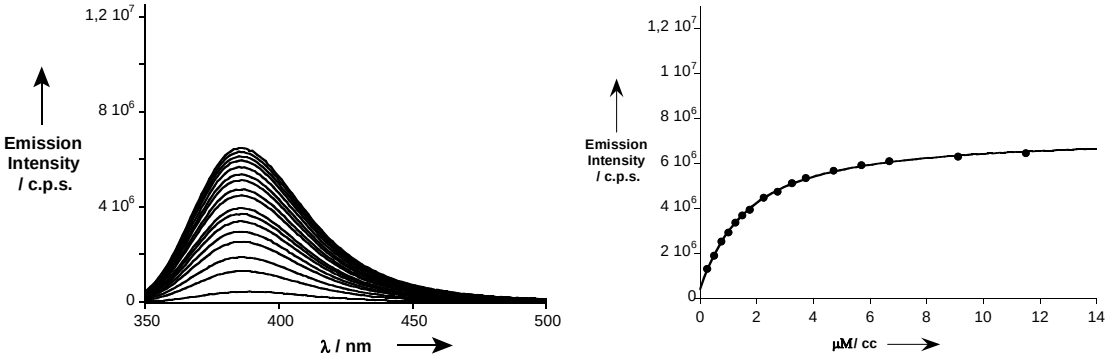

Figure S34. *Oligonucleotide* **AATT**. **Left**: fluorescence emission spectra of **11** in the presence of successive aliquots of target oligonucleotide. **Right:** Plot of the fluorescence emission at 386 nm against the total ds-DNA concentration and best-fit curve to a 1:1 binding mode. *Estimated K_D (average of three experiments): K_D= 1.9 ± 0.1 μM.*

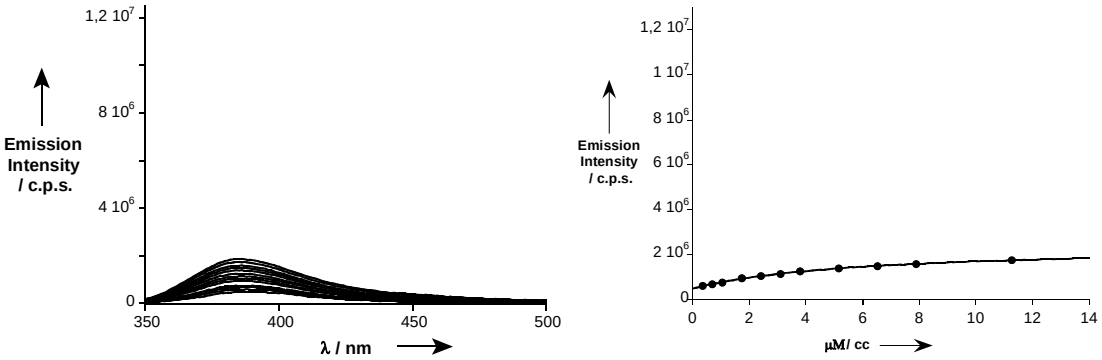

Figure S35. ***Left****: Oligonucleotide* **GGCCC**. **Left**: fluorescence emission spectra of **11** in the presence of successive aliquots of target oligonucleotides. **Right:** Plot of the fluorescence emission at 386 nm against the total ds-DNA concentration.

Fluorescence titrations of furan 12 with different DNAs.

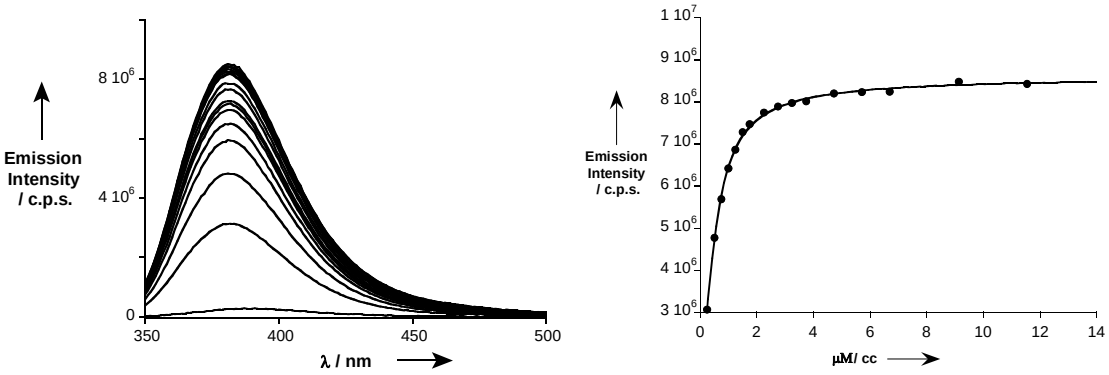

Figure S36. *Oligonucleotide* **AAATTT**. **Left**: fluorescence emission spectra of **12** in the presence of successive aliquots of target oligonucleotide. **Right:** Plot of the fluorescence emission at 386 nm against the total ds-DNA concentration and best-fit curve to a 1:1 binding mode. *Estimated K_D (average of three experiments): K_D= 246 ± 27 nM.*

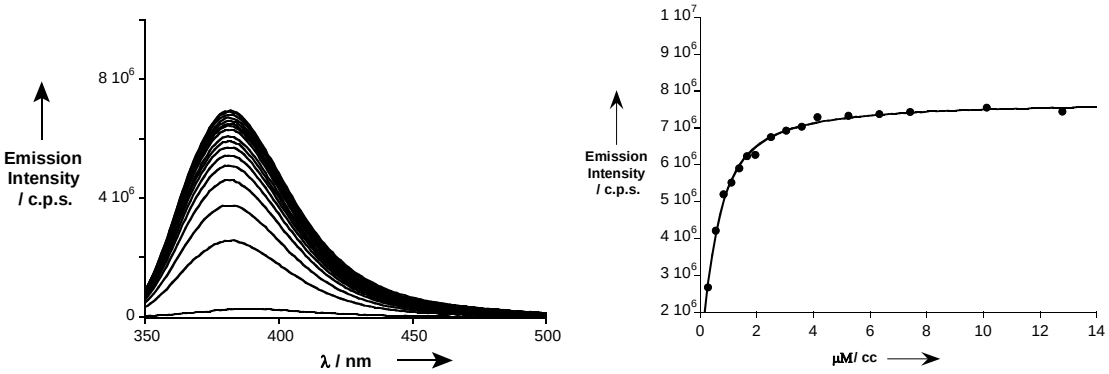

Figure S37. *Oligonucleotide* **AATTT**. **Left**: fluorescence emission spectra of **12** in the presence of successive aliquots of target oligonucleotide. **Right:** Plot of the fluorescence emission at 386 nm against the total ds-DNA concentration and best-fit curve to a 1:1 binding mode. *Estimated K_D (average of three experiments): K_D= 317 ± 43 nM.*

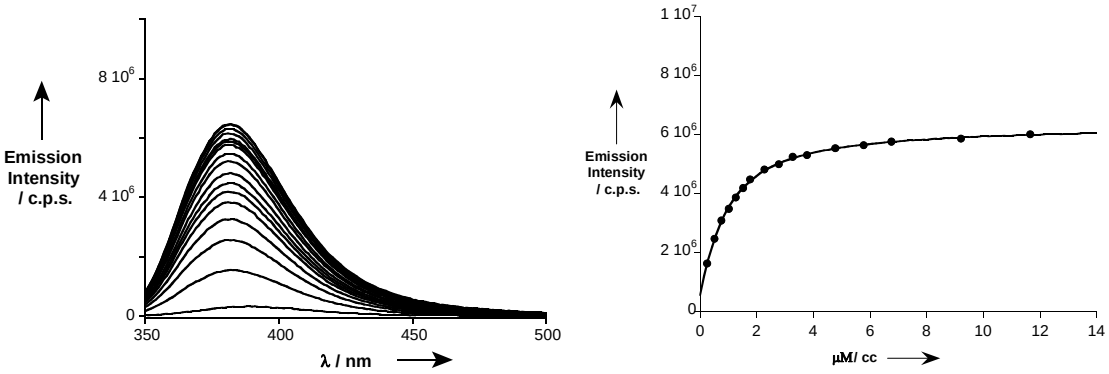

Figure S38. *Oligonucleotide* **AATT**. **Left**: fluorescence emission spectra of **12** in the presence of successive aliquots of target oligonucleotide. **Right:** Plot of the fluorescence emission at 386 nm against the total ds-DNA concentration and best-fit curve to a 1:1 binding mode. *Estimated K_D (average of three experiments): K_D= 782 ± 64 nM.*

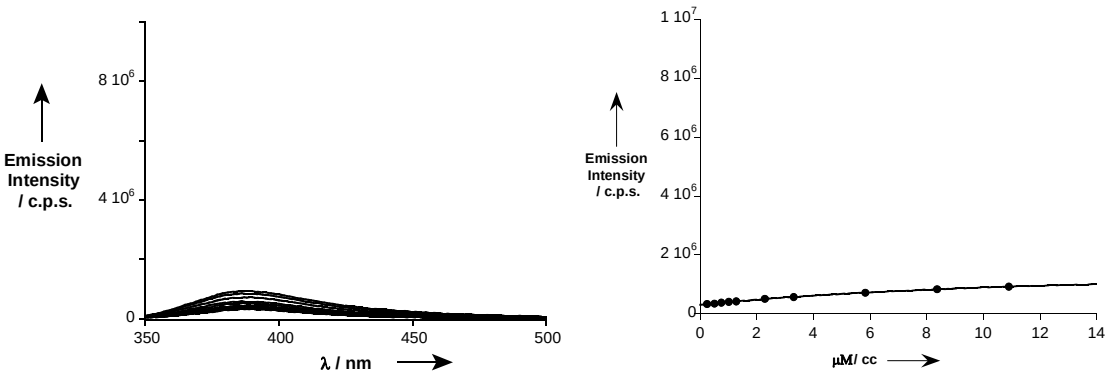

Figure S39. *Oligonucleotide* **GGCCC**. **Left**: fluorescence emission spectra of **12** in the presence of successive aliquots of target oligonucleotides. **Right:** Plot of the fluorescence emission at 386 nm against the total ds-DNA concentration.

Fluorescence titrations of azide derivative 13 with different DNAs.

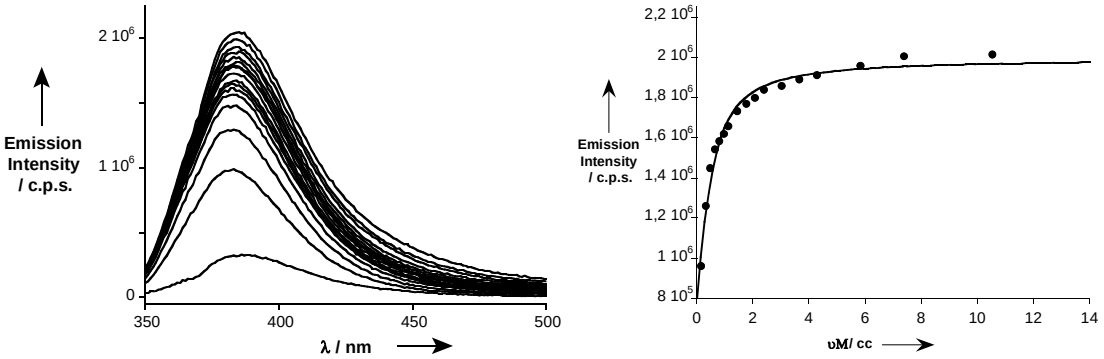

Figure S40. oligonucleotide **AAATTT**. **Left**: fluorescence emission spectra of **13** in the presence of successive aliquots of target oligonucleotide. **Right:** Plot of the fluorescence emission at 386 nm against the total ds-DNA concentration and best-fit curve to a 1:1 binding mode. *The estimated K_D value is the average of three experiments: K_D= 206 ± 21 nM.*

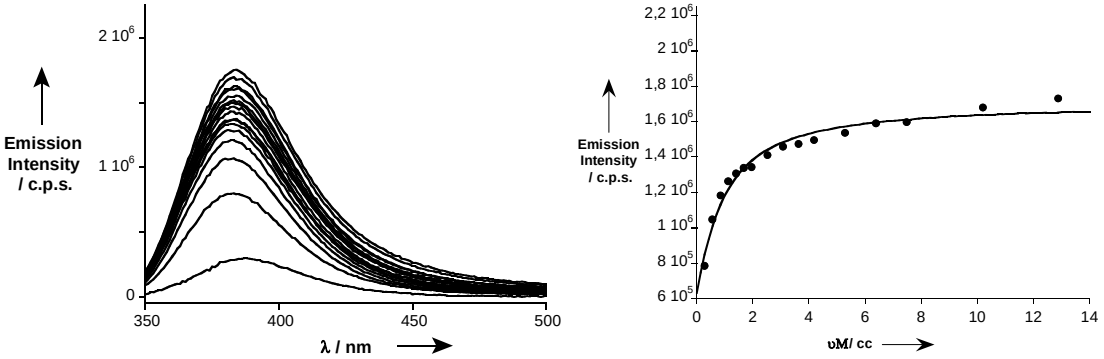

Figure S41. Oligonucleotide **AATTT**. **Left**: fluorescence emission spectra of **13** in the presence of successive aliquots of target oligonucleotide. **Right:** Plot of the fluorescence emission at 386 nm against the total ds-DNA concentration and best-fit curve to a 1:1 binding mode. *Estimated K_D (average of three experiments): K_D= 250 ± 49 nM.*

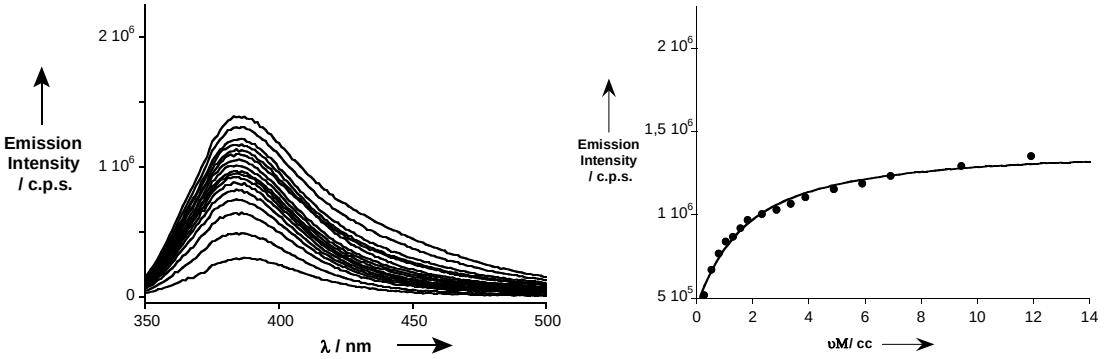

Figure S42. Oligonucleotide **AATT**. **Left**: fluorescence emission spectra of **13** in the presence of successive aliquots of target oligonucleotide. **Right:** Plot of the fluorescence emission at 386 nm against the total ds-DNA concentration and best-fit curve to a 1:1 binding mode. *Estimated K_D (average of three experiments): K_D= 362 ± 11 nM.*

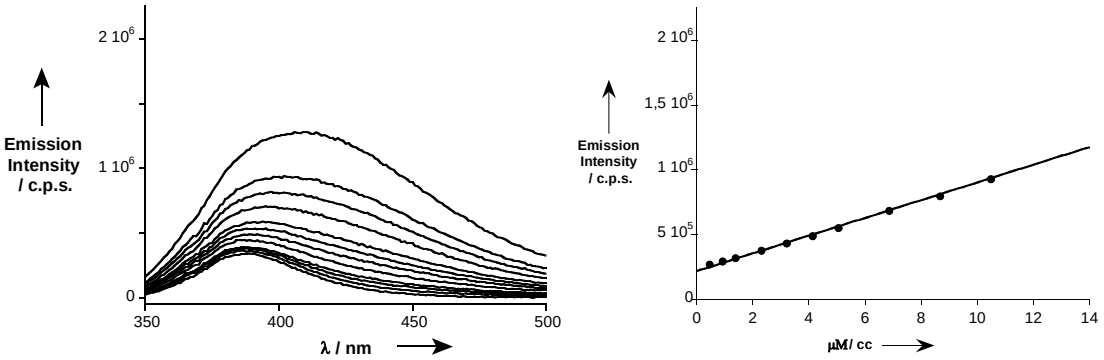

Figure S43. Oligonucleotide **GGCCC**. **Left**: fluorescence emission spectra of **13** in the presence of successive aliquots of target oligonucleotide. **Right:** Plot of the fluorescence emission at 386 nm against the total ds-DNA concentration.

Determination of binding stoichiometry by the continuous variation method (job plot)

In the continuous variation method, the total molar concentration of pyridine **10** plus DNA is held constant, but their mole fractions are varied.[2] The ratio between both mole fractions at the maximum of the Job curve is called *n*, which shows the binding stoichiometry. The first three points on each side of the curve were linearly fitted, and the intersection point of both lines gives the value of *n*. Eleven solutions of **10** and respective DNA with different mole fractions in Tris-HCl buffer 20 mM pH 7.5, 100 mM NaCl were prepared for each experiment; but keeping their total concentration in 6 μM. The sequence of the DNA was **AAGTT**: 5'−GGCG AAGTT CGC TTTTT GCGA ACTT CGCC−3'.

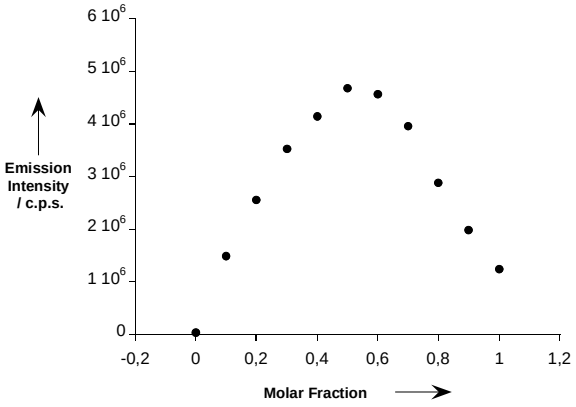

Figure S44. *Job plot experiment of **10** and **AAGTT** DNA 6 μM; n = 0.49/0.51 = 0.96.*

(2) C. Y. Huang, *Methods Enzymol.* **1982**, *87*, 509-525

Fluorescence titrations of coumarine derivative 15a.

The emission spectra was recorded from 345 nm to 650 nm.

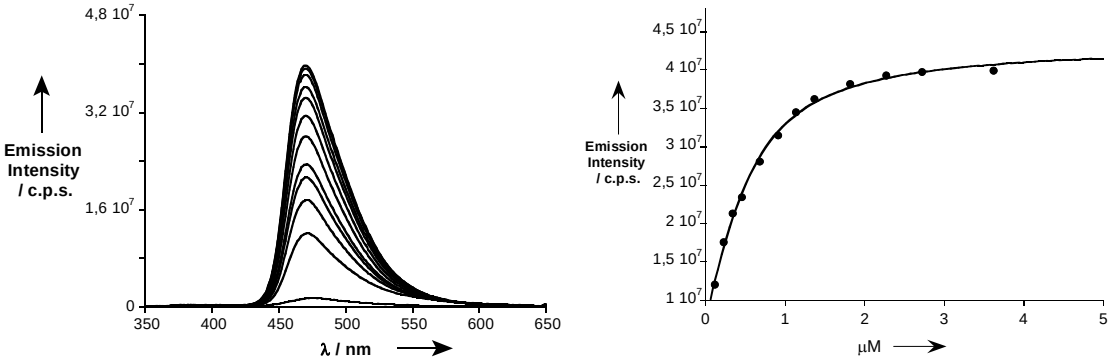

Figure S45. Oligonucleotide **AAATTT**. **Left**: fluorescence emission spectra of **15a** in the presence of successive aliquots of target oligonucleotide. **Right:** Plot of the fluorescence emission at 470 nm against the total ds-DNA concentration and best-fit curve to a 1:1 binding mode. *The estimated K_D value is the average of three experiments: K_D = 268 ± 30 nM.*

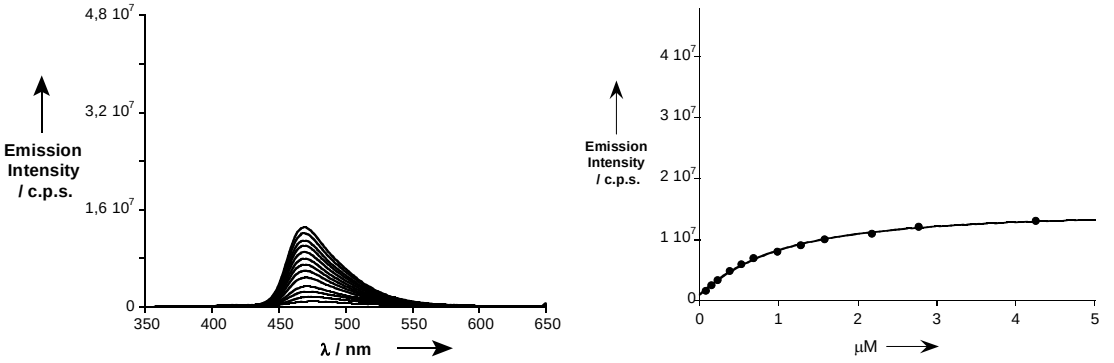

Figure S46. **Left**: Oligonucleotide **GGCCC**. **Left**: fluorescence emission spectra of **15a** in the presence of successive aliquots of target oligonucleotide. **Right:** Plot of the fluorescence emission at 470 nm against the total ds-DNA concentration and best-fit curve to a 1:1 binding mode *The estimated K_D value is the average of three experiments: K_D = 701 ± 69 nM.*

The excitation spectra of **15a**.

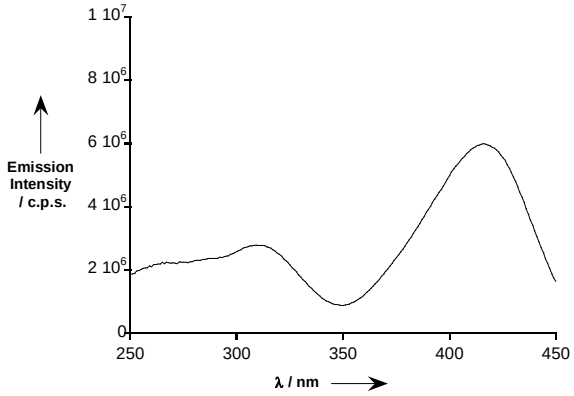

Figure S47. Excitation spectra of a 0.5 µM solution of compound **15a** in TrisHCl 20 mM pH 7.5, 100 mM of NaCl measured at 470 nm and recorded from 250 to 450 nm.

Fluorescence titrations with the arginine conjugated 15b.

With the ds-oligonucleotide equipped with the target sequence we carried out two sets of experiments, using different concentrations of the probe. At higher concentrations (A) we got a better fitting. In any case we can deduce that the Kd for this dsDNA is between 5-35 nM.

To 1 mL of a 0.5 µM solution of the compound **15b** in Tris-HCl buffer 20 mM pH 7.5, 100 mM NaCl, aliquots of a ≈ 140 µM stock solution of the respective dsDNA were successively added, and the fluorescence spectra were recorded after each addition.

In order to calculate the concentration of the peptide **15b** we used the molar extinction coefficient of compound **16**.

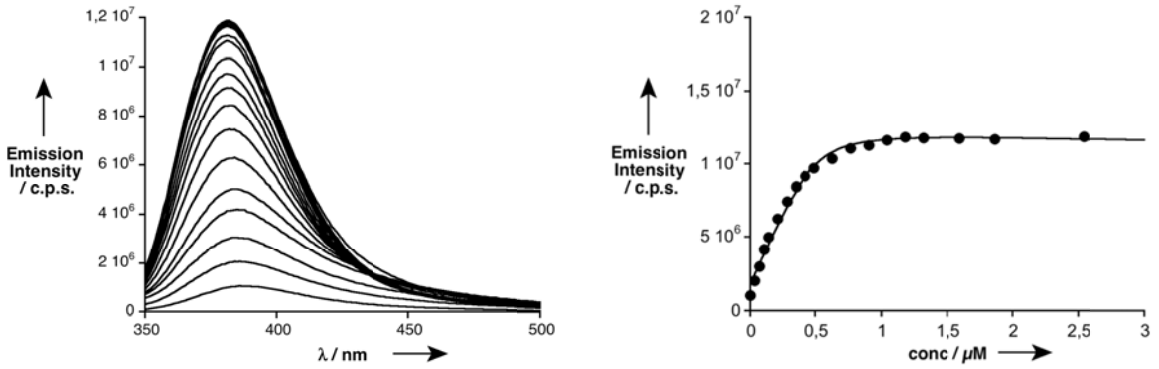

Figure S48. Left: Fluorescence spectra of the titration of the peptide **15b** with dsDNA 5`-GAC*AAATTT*GAGAGTACGCT-3´ (only one strand is shown)**. Right:** Plot o**f** the fluorescence emission at 386 nm nm against the total ds-DNA concentration and best-fit curve to a 1:1 binding mode. *The estimated K_D value is the average of three experiments: K_D= 34 ± 20 nM.*

The other set of experiments were achieved using 1 mL of a 0.075 µM solution of the compound **15b** in Tris-HCl buffer 20 mM pH 7.5, 100 mM NaCl. Aliquots of a ≈ 20 µM stock solution of the respective dsDNA were successively added, and the fluorescence spectra were recorded after each addition.

In order to calculate the concentration of the peptide **15b** we used the molar extinction coefficient of compound **16**.

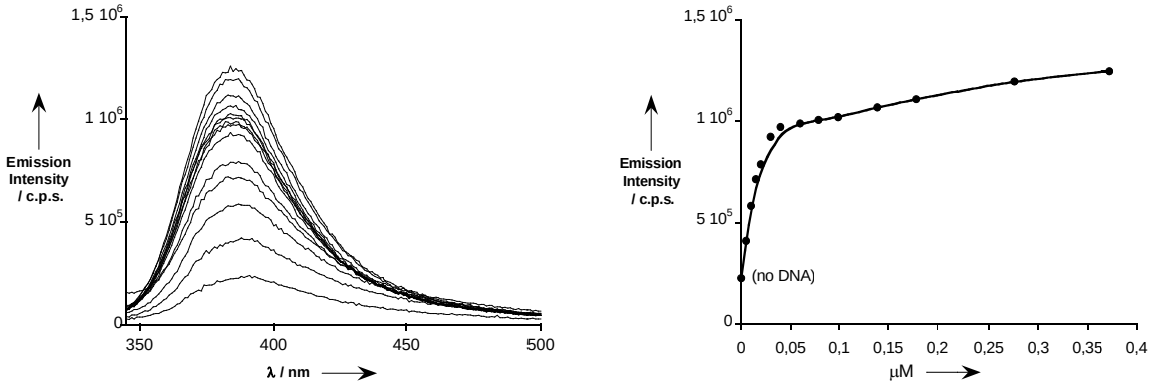

Figure S49. Left: Fluorescence spectra of the titration of the peptide **15b** with dsDNA 5`-

GAC*AAATTT*GAGAGTACGCT-3′ (only one strand is shown)**. Right:** Plot of the fluorescence emission at 386 nm nm against the total ds-DNA concentration and best-fit curve to a 1:1 binding mode. *The estimated K_D value is the average of three experiments: K_D= 5 ± 16 nM.*

With a dsDNA lacking the AT rich site:

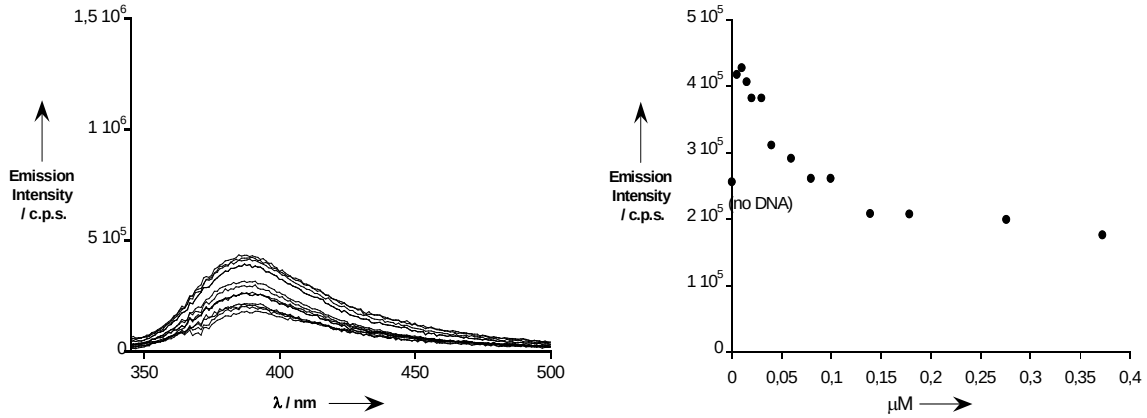

Figure S50. Left: Fluorescence spectra of the titration of the peptide **15b** with dsDNA **GC rich**: 5'−AGCGCACGTCCTGCACGTC−3', (only one strand is shown). **Right:** Plot of the fluorescence emission at 386 nm nm against the total ds-DNA concentration.

Gel Mobility Shift Assay

EMSA was performed with a *BIO-RAD Mini Protean* gel system, powered by a electrophoresis power supplies *PowerPac Basic* model, maximum power 150 V, frequency 50-60 Hz at 140 V (constant V).

Incubation binding mixtures (20 μL) contained 18 mM Tris·HCl (pH 7.5), 90 mM KCl, 1.8 mM $MgCl_2$, 1.8 mM EDTA, 9% glycerol, 0.11 mg/mL BSA and 4.4% NP-40 and 50 nM of the desired dsoligonucleotide. After incubation for 30 min the samples were loaded and run into a 10% nondenaturing polyacrylamide gel using 0.5× TBE buffer (44.5 mM Tris, 44.5 mM Boric acid, 1 mM EDTA pH 8.0) for 45 min at rt. These gels were stained with *SyBr Gold*.

Electrophoretic mobility shift assay for arginine rich peptide **15b**

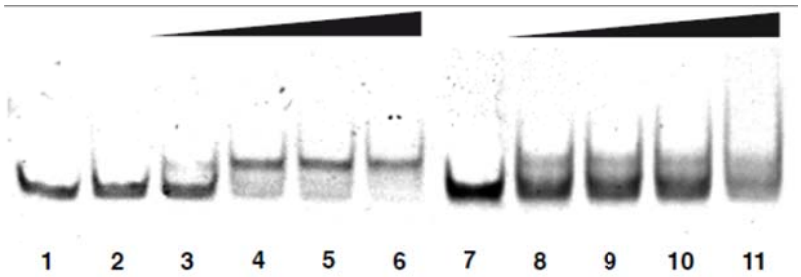

Figure S51. *EMSA results showing the binding of the peptide **15b** to dsDNAs [50 nM]. Lane 1: dsDNA* **A/T** (*5´*-GAC *AAATTT* GAGAGTACGCT-*3´*) *+ [1000 nM of* Cu^{+2}*] Lanes 2−6: dsDNA* **A/T** *+ [**15b**] = 0, 300, 400, 500, 700 nM; Lanes 7-11: dsDNA **G/C rich** 5`*-AGCGCACGTCCTGCACGTC *-3´ + [**15b**] = 0, 300, 400, 500, 700 nM. Only one strand of the dsDNA is shown.*

Control EMSA experiment with hybrid **15c** and a dsDNA in which the binding sites are not appropriately arranged.

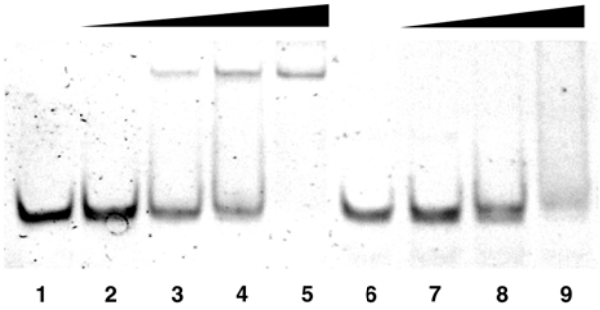

Figure S52. *Lanes 1-5, **ATF^{hs}-A/T** oligonucleotide with increasing equimolar concentrations of cJun and **15c**: 0, 250, 500, 750 and 1000 nM; lanes 6-9, oligonucleotide 5'− GAGG AAATTT ATGA CGTTCG −3' (only one strand is shown) with increasing equimolar concentrations of **15c** and **cJun**: 0, 250, 500, 1000 nM.*

Preliminary cell uptake experiments of 15a

Vero cells were maintained in DMEM (Dulbecco Modified Eagle Medium) containing 10% of FBS (Fetal Bovine Serum). Cells were seeded in twelve well plates containing glass coverslips (15 mm) the day before the uptake experiments. Cells were then washed 3 times in PBS and overlaid with 1 mL of fresh PBS with no serum added. Compound **15a** was added to a final concentration of 5 µM, and samples were incubated for 30 min at room temperature in the absence of light. After incubation, and without fixation, the coverslips were mounted on glass slides with *Mowiol 4-88*® [100 mg/mL in 100 mM Tris-HCl pH 8.5, 25% glycerol and 0.1% DABCO (as an antifading agent)]. Images were obtained with an Olympus DP-50 digital camera mounted on an Olympus BX51 fluorescence microscope equipped with a 360-370 nm excitation filter and 420 nm emission filter, and further processed (cropping and resizing, and contrast and brightness adjustment) with *Adobe Photoshop* (Adobe Systems).

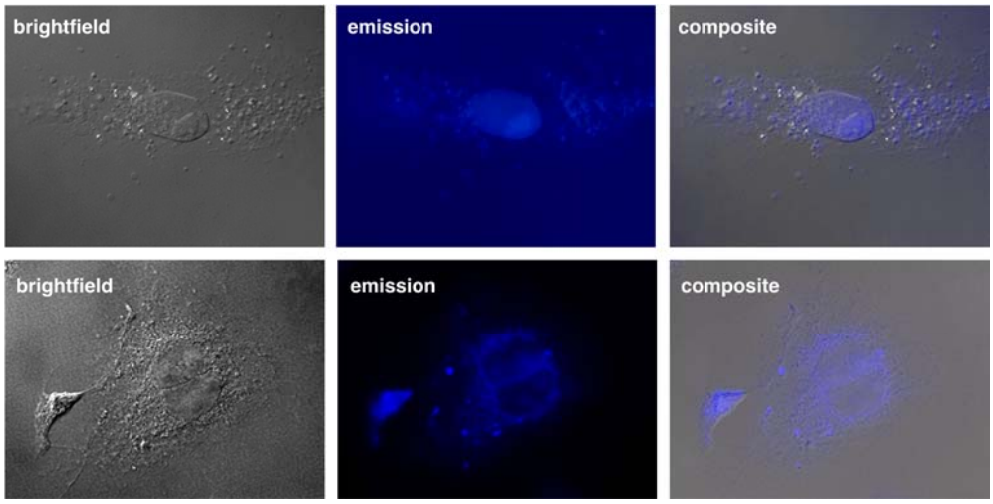

Figure S53. Top: *Vero* cells incubated with **15a** for 30 min, **Top**: Fixed cells (most staining is in the nucleus); **Bottom**: Live cells (perinuclear staining).

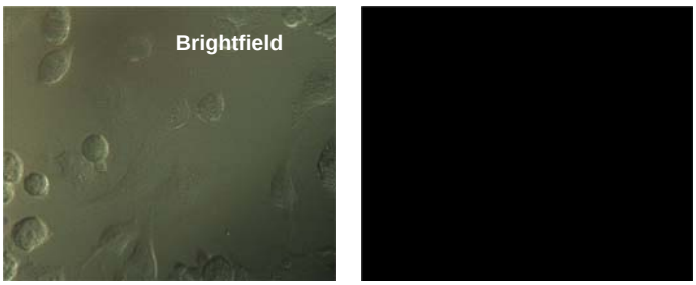

Figure S54. Control experiment, cells with no **15a** added.

Modelling

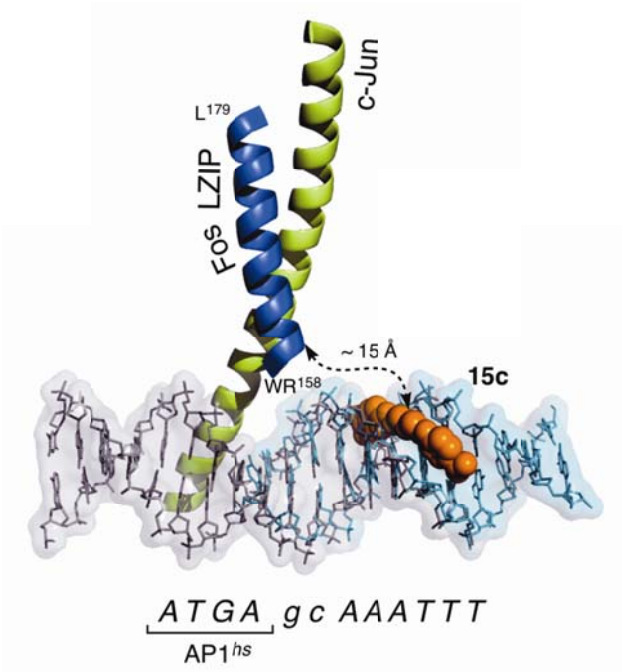

Figure S55. The design of **15c** was based on the crystal structures of both the Fos/Jun heterodimer (J. N. M. Glover, S. C. Harrison, *Nature* 1995, **373**, 257; Protein Data Bank ID: 1FOS), and pentamidine bound to their respective DNA target sequences. By superimposing the DNA backbone of both complexes with the *PyMol* Software (The PyMOL Molecular Graphics System, Version 1.30, Schrödinger, LLC) we could obtain a plausible model for the simultaneous interaction of the pentamidine in the minor groove bound to an A/T-rich sequence, and the Fos/Jun complex bound to an adjacent sequence. This crude interaction model allowed us to select the appropriate amino acid for connecting the Fos leucine zipper, and the length of the connector between the peptide and the bisbenzamidine. Given the geometry of the Fos helix, and the fact that the pentamidine binds in the minor groove of the DNA, a short "GC" spacer was introduced in the DNA sequence to allow simultaneous binding of both recognition elements on the same face of the DNA.

Curve fitting analysis

The typical equation for a 1:1 binding in which an unlabeled ligand (dsDNA) is added over a fluorescent receptor is described by the following equations, if non-specific binding is ignored:

$$K_D = \frac{R \cdot L}{C} \quad (1)$$

$$R_T = R + C \quad (2)$$

$$L_T = L + C \quad (3)$$

$$F_T = F_0 + F_C \times C \quad (4)$$

Where R is the concentration of the free receptor in the equilibrium; R_T, total receptor concentration (considered constant throughout the titration); L, concentration of the free ligand in the equilibrium; L_T, total concentration of added ligand (DNA); K_D, dissociation constant of the interaction between the receptor and the ligand; C equilibrium concentration of the ligand-receptor complex; F_T, total observed fluorescence; F_0, adjustable parameter accounting for the background fluorescence; F_C adjustable parameter for the labeled ligand-receptor complex molar fluorescence. Solving the system for F_T and eliminating R, L, and R_L, we obtain the well-known equation 5.

$$F_T = \frac{1}{2}[2F_0 + F_C\sqrt{K_D^2 + (L_T - R_T)^2 + 2K_D(L_T + R_T)})] \quad (5)$$

If minor, non-specific binding of the probe to the DNA is considered, it is better to use an equation in which the total fluorescence, F_T, takes into account this contribution, assuming that the nonspecific binding under these concentrations is nonsaturable and linearly dependent on the ligand (DNA) concentration (F_L L_T).[3]

$$F_T = F_0 + F_C \cdot C + F_L \cdot L_T \quad (6)$$

The alternative set of equations (1-3, 6) was solved using *Mathematica 6.0.1.0* for *MacOS X* (*Wolfram Research*), resulting in equation 7, which was used to fit the experimental data using non-linear regression analysis.

$$F_T = \frac{1}{2}[2F_0 + F_C \cdot K_D + F_C \cdot L_T + 2F_L \cdot L_T + F_C \cdot R_T - F_C\sqrt{K_D^2 + (L_T - R_T)^2 + 2K_D(L_T + R_T)})] \quad (7)$$

In our cases we observed that the differences in using one or other equation are minor, but we preferred to use that considering non specific contributions.

(3) M. H. A. Roehrl, J. Y. Wang, G. Wagner, *Biochemistry* **2004**, *43*, 16056.